Nickel 2-Iminopyridine *N*-Oxide (PymNox) Complexes: Cationic Counterparts of Salicylaldiminate-Based Neutral Ethylene Polymerization Catalysts

M. Brasse, J. Cámpora,* P. Palma, and E. Álvarez

Instituto de Investigaciones Químicas, Consejo Superior de Investigaciones Científicas-Universidad de Sevilla, Spain

V. Cruz and J. Ramos

GIDEM, Instituto de Estructura de la Materia, Consejo Superior de Investigaciones Científicas, Serrano 119, 28006 Madrid, Spain

M. L. Reyes

Centro de Tecnología Repsol-YPF, Carretera de Extremadura NV, Km 18, 28930 Mostoles, Madrid, Spain

Received June 12, 2008

2-Iminopyridine *N*-oxides (PymNox) constitute a promising class of ligands that can be considered as the neutral counterparts of the well-known salicylaldiminate system. A series of nickel PymNox complexes displaying different substitution patterns in the ligand have been synthesized, and their activity as ethylene polymerization catalysts has been studied. While an electron-donor group (OMe) at the remote position 4 of the pyridine ring causes a moderate decrease of the catalytic activity and increase of the polyethylene molecular weight, a strongly electron-withdrawing group (NO_2) in this position shifts the catalyst selectivity from ethylene polymerization to oligomerization. The introduction of a phenyl substituent next to the pyridine nitrogen (position 6) causes a significant increase of the catalytic activity and the polymer molecular weight. Although aldimino PymNox catalysts are inactive in ethylene−methyl acrylate copolymerization, we observed that acetaldimino (displaying the Me-C═NAr group) catalysts display a small but significant activity on this account, giving rise to copolymers incorporating ca. 1% methyl acrylate in their structure. The trends observed in the PymNox catalytic system are strongly reminiscent of those of nickel salicylaldiminates (although the former are considerably more active), demonstrating for the first time that substitution of the widely used phenoxo anionic group by the neutral pyridine *N*-oxide fragment is a useful possibility in the design of late transition metal catalysts for olefin polymerization.

Introduction

Much of the interest that has arisen in recent years by late transition metal-based olefin polymerization catalysts stems from their tolerance to polar molecules, which in some cases enables controlled copolymerization of neutral and polar comonomers.[1] The first example of copolymerization of ethylene with methyl acrylate (a monomer of technical interest) by palladium α-diimine, reported by Brookhart in 1996,[2] triggered widespread attention to new group 10 complexes as potentially useful catalysts for the production of functionalized polyethylenes. However, these attempts met serious difficulties, since even late transition metal catalysts are often readily poisoned by such co-monomers. Experimental[3] and computational[4] investigations have uncovered a number of mechanisms for catalyst deactivation, e.g., blocking of the metal center by σ-coordination of the polar co-monomer. These have shown that palladium complexes are in general superior to those of nickel for polar co-monomer incorporation, but replacing palladium with nickel might be essential for economical reasons, if large-scale application processes are to be achieved someday. This is by no means a trivial task, which still will require extensive catalyst development.

In the design of new olefin polymerization catalysts, electric charge is probably the variable with a deeper impact on their tolerance to polar substances. Mild electrophilicity provided by electrically neutral complexes favors this kind of tolerance. The long-known capability of the neutral SHOP catalysts to oligomerize and polymerize olefins was soon recognized as a potentially useful feature in polar co-monomer incorporation.[5] Neutral nickel salicylaldiminate catalysts, first reported by Grubbs,[6] laid a new milestone in the field. These display relatively high catalytic activities in ethylene homopolymerization, are compatible with polar solvents (even aqueous media[7]), and are capable of incorporation of certain types of

* Corresponding author. E-mail: campora@iiq.csic.es.

(1) (a) Ittel, S. D.; Johnson, L. K.; Brookhart, M. *Chem. Rev.* **2000**, *100*, 1169. (b) Gibson, V. C.; Spitzmesser, S. K. *Chem. Rev.* **2003**, 103.

(2) Johnson, L. K.; Mecking, S.; Brookhart, M. *J. Am. Chem. Soc.* **1996**, *118*, 267.

(3) (a) Mecking, S.; Johnson, L. K.; Wang, L.; Brookhart, M. *J. Am Chem. Soc.* **1998**, *120*, 888. (b) Michalak, A.; Ziegler, T. *Organometallics* **2001**, *20*, 1521. (c) Kang, M.; Sen, A.; Zakharov, L.; Rheingold, A. L. *J. Am. Chem. Soc.* **2002**, *124*, 12080. (d) Foley, S. R., Jr.; Shen, A.; Jordan, R. F. *J. Am. Chem. Soc.* **2003**, *125*, 4350. (e) Waltman, A. W.; Younkin, T. R.; Grubbs, R. H. *Organometallics* **2004**, *23*, 5121. (f) Li, W.; Zhang, X.; Meetsma, A.; Hessen, B. *J. Am. Chem. Soc.* **2004**, *126*, 12246. (g) Williams, B. S.; Leatherman, M. D.; White, P. S.; Brookhart, M. *J. Am. Chem. Soc.* **2005**, *127*, 5132. (h) Groux, L. F.; Weiss, T.; Reddy, D. N.; Chase, P. A.; Piers, W. E.; Ziegler, T.; Parvez, M.; Benet-Buchholz, J. *J. Am. Chem. Soc.* **2005**, *127*, 1841. (i) Wu, F.; Foley, S. R.; Burns, C. T.; Jordan, R. F. *J. Am. Chem. Soc.* **2005**, *127*, 1841. (j) Stojcevic, G.; Prokopchuk, E. M.; Baird, M. C. *J. Organomet. Chem.* **2005**, *690*, 4349.

10.1021/om800548y CCC: $40.75
Publication on Web 08/27/2008

Chart 1. Representation of the Propagating Species in the Neutral Grubbs Salicylaldiminate-Based Catalyst System (A) and the Neutral PymNox Catalysts (B)

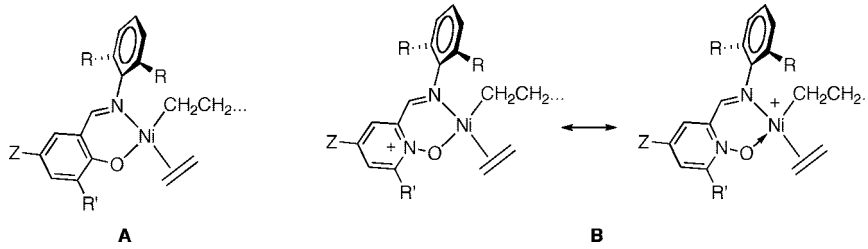

A **B**

Scheme 1

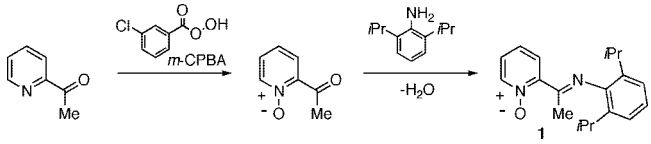

functional monomers.[8] More recently, other electrically neutral group 10 catalysts have been successfully allowed co-polymerization of ethylene and acrylic monomers.[9−12] However, achieving high polymerization activities usually demands more electrophilic, cationic metal centers. An obvious approach to solve this dilemma is to adopt a compromise allowing a fractional positive charge to sit at the metal center. We reasoned that a modification of the original Grubbs' salicylaldiminate catalyst design (Chart 1, **A**) by replacing the anionic aryloxide moiety by a neutral pyridine *N*-oxide fragment would lead to highly active cationic polymerization catalysts, while it could maintain to some degree their tolerance to polar substances. This substitution leads to the isostructural 2-iminopyridine *N*-oxide (PymNox) family of ligands (**B**). It may be anticipated that the *N*-oxide fragment might contribute to efficiently delocalize part of the positive charge on the ligand,[13] leading to an intermediate situation between typically cationic and neutral polymerization catalysts. This concept is not new: Dyker[14] has previously relied on it for the design of a neutral analogue of Jacobsen's Salen ligand, and Erker has recently reported the synthesis of a number of PymNox ligands and the corresponding complexes of Ni, Pd, Co, and Cu, hinting at their potential in homogeneous catalysis.[15] However, this potential remains largely undeveloped and in the case of olefin polymerization is still unexplored. In this contribution, we begin our study of PymNox complexes and their behavior as ethylene polymerization catalysts, providing some preliminary results on the capability of these compounds to copolymerize ethylene with methyl acrylate.

Results and Discussion

Synthesis of PymNox Ligands. *N*-Oxides of pyridine and their derivatives are usually prepared by oxidation of the corresponding heterocycles. Peroxocarboxylic acids, particularly *m*-chloroperbenzoic acid (*m*CPBA), are the reagents of choice for this kind of transformation. As previously shown by Erker,[15] 2-acetylpryridine is oxidized in this fashion to afford the corresponding oxide (Scheme 1). The sensitive aldehyde group of pyridine-2-carbaldehyde does not survive these oxidation conditions, and a different approach must be used in order to obtain the corresponding *N*-oxide. Selective oxidation of the methyl group of 2-picoline *N*-oxide (readily obtained from 2-picoline) by selenium dioxide in pyridine under reflux provides an adequate method to obtain the required compound (Scheme 2).[16] 2-Acetyl and 2-carbaledehyde pyridine *N*-oxide derivatives were condensed with 2,6-diisopropylaniline in a Dean-Stark apparatus to afford ligands **1** and **2**.

The presence of bulky substituents at position 6 of the central aryl group is a crucial feature of salicylaldiminate nickel polymerization catalysts, to achieve high catalytic activities.[17] An extension of the method for compound **2** was used for the synthesis of the quinoline derivative **3** and ligand **4**, the latter bearing a phenyl substituent at position 6 in the pyridine ring. Pyridines displaying bulky substituents at the neighboring ring positions are often difficult to oxidize,[14,18] but somewhat surprisingly, this step proceeds readily in both cases, especially for **3**.

Scheme 2 also shows the preparation of the starting material required for **4**, 2-phenyl-6-methylpyridine. The key step is a Kumada coupling reaction using 2-bromo-6-methylpyridine,

(4) (a) Philipp, D. M.; Muller, R. P.; Goddard, W. A., III; Storer, J.; McAdon, M.; Mullins, M. *J. Am. Chem. Soc.* **2002**, *124*, 10198. (b) Michalak, A.; Ziegler, T. *Organometallics* **2003**, *22*, 2069. (c) Michalak, A.; Ziegler, T. *Organometallics* **2003**, *22*, 2660. (d) Deubel, D. V.; Ziegler, T. *Organometallics* **2003**, *22*, 2660. (e) Szabo, M. J.; Jordan, R. F.; Michalak, A.; Piers, W. E.; Weiss, T.; Yang, S.-Y.; Ziegler, T. *Organometallics* **2004**, *23*, 5565.

(5) (a) Klabunde, U.; Mulhaupt, R.; Herskovitz, T.; Janowicz, A. H.; Calabrese, J.; Ittel, S. D. *J. Polym. Sci., Part A: Polym. Chem.* **1987**, *25*, 1989. (b) Klabunde, U.; Ittel, S. D. *J. Mol. Catal.* **1987**, *41*, 123. (c) Klabunde, S. U.S. Patent 4716205, 1987.

(6) (a) Wang, C. M.; Friedrich, S.; Younkin, T. R.; Li, R. T.; Grubbs, R. H.; Bansleben, D. A.; Day, M. W. *Organometallics* **1998**, *17*, 3149. (b) Younkin, T. R.; Connor, E. F.; Henderson, J. I.; Friedrich, S. K.; Grubbs, R. H.; Bansleben, D. A. *Science* **2000**, *287*, 460.

(7) (a) Bauers, F. M.; Mecking, S. *Macromolecules* **2001**, *34*, 1165. (b) Bauers, F. M.; Mecking, S. *Angew. Chem. Int. Ed.* **2001**, *40*, 3020. (c) Korthals, B.; Göttker-Schnetmann, I.; Mecking, S. *Organometallics* **2007**, *26*, 1311. (d) Göttker-Schnetmann, I.; Wehrmann, P.; Röhr, C.; Mecking, S. *Organometallics* **2007**, *26*, 2348. (e) Mecking, S.; Held, A.; Bauers, F. M. *Angew. Chem., Int. Ed.* **2002**, *41*, 544.

(8) Connor, E. F.; Younkin, T. R.; Henderson, J. I.; Hwang, S.; Grubbs, R. H.; Roberts, W. P.; Litzau, J. J. *J. Polym. Sci. A* **2002**, *40*, 2842.

(9) (a) Drent, E.; van Dijk, R.; van Ginkel, R.; van Oort, B.; Pugh, R. I. *Chem. Commun* **2002**, 744. (b) Weng, W.; Shen, Z.; Jordan, R. F. *J. Am. Chem. Soc.* **2007**, *129*, 15450.

(10) (a) Kochi, T.; Yoshimura, K.; Nozaki, K. *Dalton Trans.* **2001**, 25. (b) Nakamura, A.; Munakata, K.; Kochi, T.; Nozaki, K. *J. Am. Chem. Soc.* **2008**, *130*, 8128.

(11) Li, X.-F.; Li, Y.-G.; Li, Y.-S.; Chen, Y.-X.; Hu, N.-H. *Organometallics* **2005**, *24*, 2502.

(12) (a) Diamanti, S. J.; Khanna, V.; Hotta, A.; Coffin, R. C.; Yamakawa, D.; Kramer, E. J.; Fredrickson, G. H.; Bazan, G. C. *Macromolecules* **2006**, *39*, 3270. (b) Coffin, R. C.; Diamanti, S. J.; Hotta, A.; Khanna, V.; Kramer, E. J.; Fredrickson, G. H.; Bazan, G. C. *Chem. Commun.* **2007**, 3350. (c) Rojas, R. S.; Barrera Galland, G.; Wu, G.; Bazan, G. C. *Organometallics* **2007**, *26*, 5339.

(13) (a) Albini, A.; Pietra, S. *Heterocyclic N-Oxides*; CRC Press: Boca Raton, FL, 1991. (b) Katritzky, A. R.; Lagowski, J. M. *Chemistry of Heterocyclic-N-oxides*; Academic Press: London, 1971.

(14) Dyker, G.; Hölzer, B.; Henkel, G. *Tetrahedron* **1999**, *10*, 3297.

(15) Nienkemper, K.; Kotov, V. V.; Kehr, G.; Erker, G.; Fröhlich, R. *Eur. J. Inorg. Chem.* **2006**, 366.

(16) Jerchel, D.; Heider, J.; Wagner, H. *Justus von Liebig Ann. Chem.* **1958**, *613*, 153.

(17) Connor, E. F.; Younkin, T. R.; Henderson, J. I.; Waltman, A. W.; Grubbs, R. H. *Chem. Commun.* **2003**, 2272.

(18) Mongin, O.; Rocca, P.; Thomas-dit-Dumont, L.; Trécourt, F. M. A. G. F.; Quéguiner, G. *J. Chem. Soc., Perkin Trans. 1* **1995**, *19*, 2503.

Scheme 2

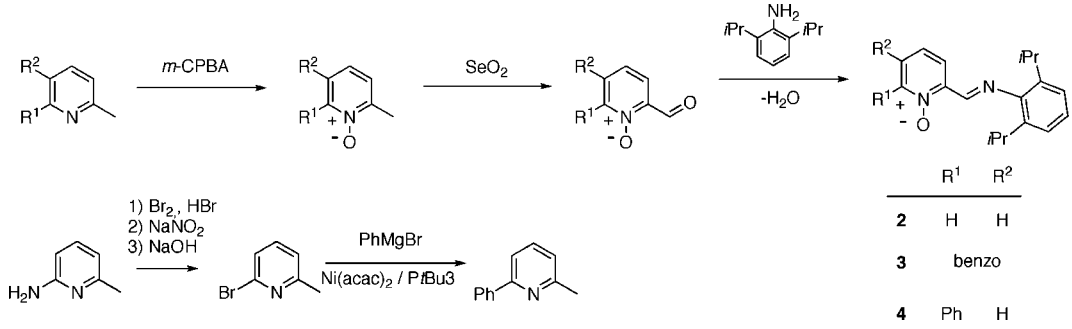

Scheme 3

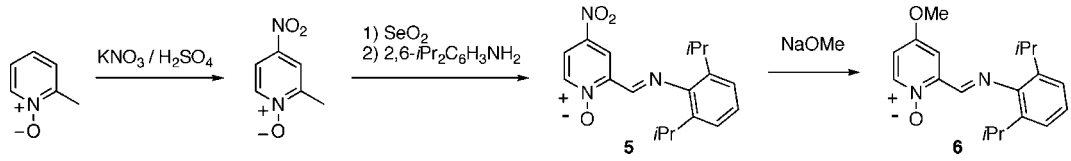

previously described by Braunstein.[19] Even though 2-bromo-6-methylpyridine was obtained in one step by selective monomethylation of 2,6-dibromopyridine with methyllithium,[20] we found the method described by Schubert et al. more advantageous. The latter relies on a diazotation of a commercially available precursor, 2-amino-6-methylpyridine.[21]

In addition to the mentioned steric effects, electron-attracting (NO_2) and -releasing groups (OMe) at position 4 in the aromatic ring of the salicylaldiminato ligands have a dramatic effect on the activity of the corresponding nickel catalysts.[7] In order to investigate the occurrence of similar electronic effects in the PymNox system, we were interested in preparing ligands displaying the same substitution pattern in the pyridine ring. Fortunately, pyridine *N*-oxides are prone to a wide variety of both electrophilic and nucleophilic substitution reactions,[13] which considerably simplified our task. 2-Picoline *N*-oxide is readily and selectively nitrated at the 4 position using a procedure adapted from the literature,[22] as illustrated in Scheme 3. The same methods described above allowed the transformation of 4-nitro-2-picoline into **5**. The methoxy derivative **6** was directly accessible from **5**, by nucleophilic displacement of the nitro group with sodium methoxide.

The electronic structure of pyridine *N*-oxides, and therefore their ability to coordinate and stabilize metal complexes, is strongly influenced by the substituents attached to the heterocyclic ring.[13] It is expected that the influence of these groups could correlate to some extent with certain spectroscopic parameters, such as the IR ν(N−O) band frequency or the intramolecular bond distances. Reliable identification of the *N*-oxide absorption is difficult because it occurs at 1200−1300 cm^{-1}, a spectral region populated with many other bands. In spite of this, we have attempted an assignation of these bands on the basis of their medium to strong intensity and comparisons between the different spectra for consistency. In a further effort to characterize the properties of ligands **1**−**6**, their crystal structures have been determined. An ORTEP view of compound **2** in shown in Figure 1, and full lists of bond lengths and angles for all the remaining ligands are provided as Supporting Information. The structure of ligand **1** was previously reported by Erker.[14] The six molecules were found in the same

Table 1. IR and Structural Data for Compounds 1−6

			bond distances (Å)[a]				
	R/Z/R′[b]	ν(N−O) cm^{-1}	N1−O1	C1−C2	C1═N2	ring av[c]	ring av SD[d]
5	H/NO_2/H	1275	1.290(2)	1.469(2)	1.265(2)	1.374	0.01
3	benzo/H/H	1245	1.292(1)	1.466(1)	1.273(1)	1.394	0.03
4	Ph/H/H	1250	1.296(2)	1.462(2)	1.255(2)	1.363	0.006
1	H/H/Me	1255	1.303(2)	1.493(2)	1.277(2)	1.379	0.01
2	H/H/H[e]	1250	1.306(2)	1.460(3)	1.265(3)	1.374	0.01
6	H/OMe/H	1250	1.310(7)	1.444(9)	1.247(8)	1.365	0.02

[a] See Figure1 numbering scheme. [b] See Chart2. [c] Average of the pyridine C−C and C−N bonds. [d] Standard deviation of the ring bond average. [e] Average distances for two crystallographically independent molecules.

configuration, with the C═N bond pointing outward from the N−O group and with the imino and the heterocyclic moieties lying in an approximately coplanar position. The only significant deviation from planarity is found for ligand **1**, where the imino group and the pyridine *N*-oxide fragment adopt a dihedral angle of 40.8° in order to avoid steric repulsions. Additional metric parameters are listed in Table 1, together with the corresponding ν(N−O) frequencies.

The electronic structures of heteroaromatic *N*-oxides have often been explained in terms of mesomeric structures; some of them are represented in Chart 2. Electron-releasing substituents in the 2, 4, or 6 position favor the localization of partial negative charge on the oxygen atom of the oxide, decreasing the N−O bond order (form **A**), while electron-withdrawing groups produce the opposite effect (form **C**). Groups 2-formylimi-

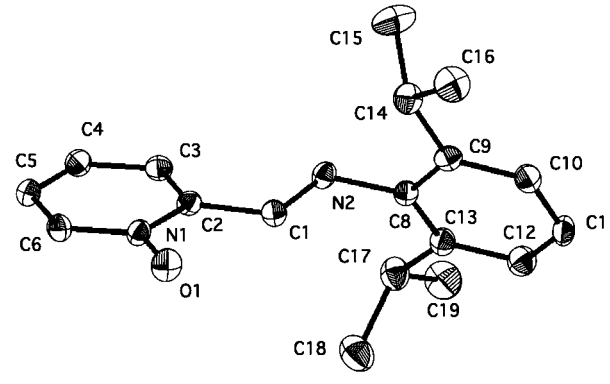

Figure 1. ORTEP view of the crystal structure of compound **2**.

(19) Speiser, F.; Braunstein, P. *Organometallics* **2004**, *23*, 3373.
(20) Basu, B.; Frejd, T. *Acta Chim. Scand.* **1996**, *50*, 316.
(21) Schubert, U. S.; Eschbaumer, C.; Hellert, M. *Org. Lett.* **2000**, *2*, 3373.

Chart 2

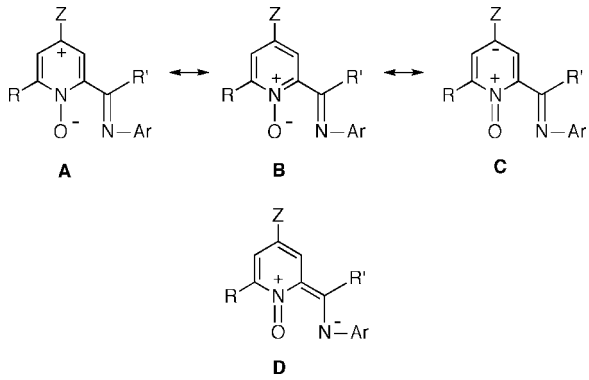

no and acetaldimino are also electron-withdrawing, and their effect can be described by form **D**. Increasing the negative charge on the oxygen makes the pyridine *N*-oxide more akin to an anionic phenoxide fragment, enhancing its donor properties. Since the N−O bond order is related to the relative weights of forms **A** and **C**, the frequencies of the IR ν(N−O) bands are expected to decrease on going from the less to the more electron-rich ligands, while the N−O bond lengths are expected to display the opposite trend.

The expected trends are approximately matched by the ligands. Thus, ligand **5**, with a strongly electron-withdrawing group (NO_2), has the higher ν(N−O) frequency and shorter N−O distance, while **6**, with the electron-donor methoxy OMe substituent, is at the opposite extreme of the series. However, variation of these parameters is less pronounced in the remaining compounds. Frequencies of the IR ν(N−O) bands were found to be virtually identical for **4**, **3**, and **6**, and the range of N−O bond lengths is only 0.02 Å wide. The latter suggests that the methoxy-substituted derivative **6** is actually similar to the unsubstituted ligand **2**, while compounds **3** and **4**, bearing mild electron-withdrawing aryl groups, are closer to **5**. The shape of the pyridine ring confirms that electronic effects have little influence on the ligand structure. Mesomeric forms **A** and **C** suggest that such effects might cause some degree of bond alternation in the six C−C and C−N distances of the heteroaromatic ring; however these are quite similar in almost all cases. As can be seen, the standard deviation of the average C−C/C−N bond length remains small and almost the same for five of the six compounds. The ring displays a somewhat less regular shape in **3** due to the presence of the fused benzo ring of the quinoline system. Bond lengths within the imino moiety are also very similar from one ligand to the other, except for **1**, where the C1−C2 bond is significantly longer, probably due to the lack of coplanarity of this group and the heteroaromatic fragment causes a lesser degree of electronic conjugation.

Syntheses of PymNox Complexes. Nickel halocomplexes **Ni1**−**Ni6** are readily prepared in good yields by treatment of $NiBr_2$(dme) (dme = 1,2-dimethoxyethane) with a slight excess of the corresponding ligand in dichloromethane, followed by precipitation with hexane (Scheme 4). They were isolated as red-brown (**Ni1**, **Ni2**, **Ni5**, **Ni6**), pink (**Ni4**), or green (**Ni3**) solids. They are all high-spin, with $\mu_{eff} = 2.9-3.5\ \mu_B$ at room temperature. In general they are quite stable and can be handled under air except for the nitro complex **Ni5**, which decays on exposure to moist air. Their IR spectra display a medium to strong absorption assigned to ν(N−O) in the proximity of 1200 cm^{-1}. The ca. 40 cm^{-1} shift to lower frequency (as compared to the free ligands) is consistent with a significant loss of the N−O π-bonding. This shift is less pronounced for the nitro-substituted complex **Ni5** ($\Delta\nu = 20\ cm^{-1}$) and largest for the methoxy-bearing derivative **Ni6** ($\Delta\nu = 58\ cm^{-1}$), confirming that electron-donor groups favor a stronger interaction of the ligand with the metal center.[23] The composition of **Ni1**−**Ni6** contrasts with those of the complexes reported by Erker, which display an additional ligand, either a solvent molecule (THF) or a second, monodentate ligand unit.[14] The crystal structure of complex **Ni1**, shown in Figure 2, shows that in this case nickel achieves pentacoordination by formation of a dimeric molecule bridged by bromide ligands. The metal center is found in a distorted square-pyramidal environment, with the basal Ni−Br2′ distance (2.5708(3) Å) being appreciably longer than Ni−Br1 and Ni−Br2 (2.4356(3) and 2.4506(3) Å, respectively). The Ni−O distance, 1.9774(12) Å, is slightly longer than in nickel salicylaldiminate complexes (ca. 1.91 Å),[24] but the difference is small, considering the different coordination number of nickel in the two complexes. As compared with the free ligand, the effect of coordination is more evident in the N1−O1 bond, which elongates by 0.023 Å, than in the imine C1═N2 bond, which is increased by only 0.01 Å. In contrast with the nickel salicyladiminate complexes, which invariably display strictly planar structures, the PymNox chelate adopts a folded configuration. Since the N2═C1−C2−C3 dihedral angle is not very different in the complex and in the free ligand (ca. 27°), this effect can be in part attributed to the natural tendency of the ligand to twist in order to avoid steric interactions between the imine methyl and the pyridine ring. However, the even wider dihedral angle Ni−O1−N1−C2 (52.3°) suggests that the chelate ring system is inherently more flexible than that of the salicyladiminate complexes.

In spite of their paramagnetic character, complexes **Ni1**, **Ni3**, and **Ni4** exhibit useful ^{1}H NMR spectra at room temperature, which have been assigned on the basis of the signal intensities and width. All the signals could be located, except for that of the aldimino H atom of **Ni3** and **Ni4**. At room temperature, the spectra of the remaining nickel compounds show very broad signals that are difficult to assign, presumably due to the occurrence of fluxional processes. Rapid exchange also occurs in the case of **Ni1**, whose ^{1}H spectrum is simpler than expected on the basis of its solid-state structure, displaying a single set of isopropyl signals. The isopropyl methyl groups are diastereotopic, indicating that this apparent simplicity is not due to the rapid rotation of the aryl groups, but probably involves either a rapid exchange of the apical and bridging bromide ligands or dimer dissociation. The situation is the same in **Ni4**, but somewhat surprisingly, **Ni3** shows a more complex ^{1}H NMR spectrum, with two independent sets of *i*-Pr signals, which suggests that a dimeric structure is rigidly maintained in solution in this case.

In contrast with the facile formation of the nickel derivatives, the PymNox ligands fail in general to react with common palladium precursors such as $Pd(MeCN)_2$ or $PdCl_2$(cod) at room temperature. However, ligand **4** reacts directly with $PdCl_2$ in warm (40 °C) acetonitrile,[14] affording **Pd4** as a yellow diamagnetic compound, whose ^{1}H and $^{13}C\{^1H\}$ NMR spectra

(22) Trécourt, F.; Gervais, B.; Mongin, O.; Gal, C. L.; Quéguiner, G. *J. Org. Chem.* **1998**, *63*, 2892.

(23) (a) Garvey, R. G.; Nelson, J. H.; Ragsdale, R. O. *Coord. Chem. Rev.* **1968**, *3*, 375. (b) Orchin, M.; Schmidt, J. *Coord. Chem. Rev.* **1968**, *3*, 345. (c) Karayannis, N. M.; Oytlewski, L. L.; Mikulski, C. M. *Coord. Chem. Rev.* **1973**, *11*, 932.

(24) (a) Zuideveld, M. A.; Wehrmann, P.; Rûhr, C.; Mecking, S. *Angew. Chem. Int. Ed.* **2004**, *43*, 869. (b) Chen, Q.; Yu, J.; Huang, J. *Organometallics* **2007**, *26*, 617. (c) Hu, T.; Li, Y.-G.; Liu, J.-Y.; Li, Y.-S. *Organometallics* **2007**, *26*, 2609.

Scheme 4

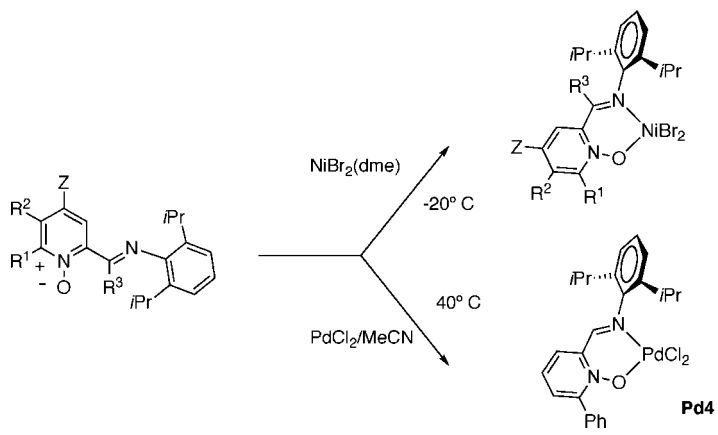

	R1	R2	R3	Z
Ni1	H	H	Me	H
Ni2	H	H	H	H
Ni3	benzo		H	H
Ni4	Ph	H	H	H
Ni5	H	H	H	NO_2
Ni6	H	H	H	OMe

are fully consistent with the proposed structure. The less ready formation of the palladium complexes suggests that the PymNox ligands bind less strongly the softer Pd(II) center than the Ni(II) ion. This is apparently supported by the smaller coordination frequency shift of the ν(N−O) band observed for **Pd4** (1230 cm^{-1}, $\Delta\nu = 25\ cm^{-1}$) than for its Ni analogue ($\Delta\nu = 46\ cm^{-1}$).

Ethylene Polymerization with PymNox Complexes. On treatment with MMAO or diethylaluminum chloride (DEAC), all PymNox nickel complexes become active ethylene polymerization or oligomerization catalysts. In contrast, the palladium complex **Pd4** is found to be inactive under these conditions. Table 2 collects activity data for these catalysts, and polymer characterization data are displayed in Table 3. All experiments were carried out in Fisher-Porter glass reactors with magnetic stirring, immersed in a water thermostatic bath. The reactor, charged with solvent and catalyst under N_2 atmosphere, was flushed three times with ethylene and allowed to stabilize at the selected pressure and temperature before starting the experiment by injection of the co-catalyst solution through a septum-capped port. Isobaric ethylene consumption was continuously monitored along the experiments. In some of them, the reactor was also equipped with a thermocouple probe in order to record changes in the internal temperature. Figure 3 shows a typical activity−temperature profile, corresponding to entry 9 of Table 2. As can be seen, the temperature curve parallels that of the catalytic activity, the latter calculated from ethylene consumption data. In general, catalytic activity reaches a maximum about 3−10 min after the beginning of the experiment, which is followed by a smooth decay. These features can be analyzed to provide some parameters that can be used to give a description of the experiments in a qualitative context. While the time elapsed until the activity peak is attained can be linked to the rate of catalyst activation, the height of the maximum measures the optimum catalyst performance under the given experimental conditions. On the other hand, the declining part of the activity curve can be approximately fitted by an exponential function, providing apparent half-life times for the catalyst that can be considered an indication of catalyst stability. The three parameters (maximum activity, time at which it occurs, and catalyst half-life) are collected in Table 2. In addition, the activity curves provide an accurate indication of how long the catalyst remains active in each experiment, and this time rather than the actual duration of the experiment,[25] has been used to calculate the average activity of the catalyst.

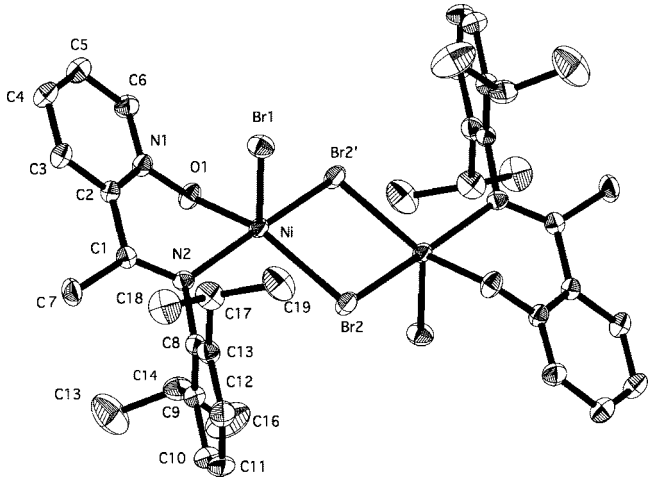

Figure 2. ORTEP view of compound **Ni1**. Selected bond distances (Å) and angles (deg): N1−O1, 1.3258(17); C2−C1, 1.486(2); C1−N2, 1.286(2); Ni−O1, 1.9774(12); Ni−N2, 2.0911(13); Ni−Br1, 2.4356(3); Ni−Br2, 2.4506(3); Ni−Br2′, 2.5708(3); Ni−O1−N1, 114.82(9); N2−C1−C2-N1, 29.06; Ni−O1−N1−C2, 52.34.

Catalysts **N1** and **Ni2** produce similar low molecular weight polyethylenes ($M_n \approx 1000-2000$) with small polydispersity indexes of 1.2−1.7. GC analyses of the reaction mixtures reveal the presence of oligomers with a flat Flory−Schulz molecular weight distribution ($\alpha \approx 0.85$), which is consistent with the low molecular weight fraction of the polymer rather than a differentiated oligomeric product. The NMR spectra of the polymer produced by **Ni1** indicate that this is more branched than that obtained with **Ni2**. This is also reflected in the T_m and crystallinity indexes indicated in the DSC data that are lower for the former catalyst. Higher productivities are achieved with catalyst **Ni2** than with **Ni1**, although the recorded catalytic activities show a different dependency on the cocatalyst dosage. The latter benefit of high amounts of cocatalyst, while the former has a performance optimum for an Al/Ni ratio of 750. In both cases, there is a direct relationship between the Al/Ni ratio and the height of the catalytic activity maximum, suggesting that the efficiency of the catalyst activation process might be a limiting factor for the recorded activities. In the case of **Ni2**, the productivity falls at the higher MMAO concentrations, which appears to be due to shorter catalyst decay times (entry 6, Table 2). However, at difference with other catalysts in this study (see below), **Ni1** and **Ni2** are fairly tolerant to high Al/Ni ratios. Interestingly, attempts to activate **Ni2** with DEAC caused

(25) The experiment duration was set to 20−25 min in most cases. Shorter times were taken when the catalyst activity was observed to drop to an inappreciable level (less than 90−95% of the initial activity).

Table 2. Ethylene Polymerization Experiments

	exptl conditions[a]							results						
entry	cat. no.	R/Z/R′[b]	[Ni] μM[c]	[Ni]/[Al][d]	time (min)	press (bar)	ext temp (°C)[e]	max. temp (°C)[f]	PE yield (grs)	av activ[g]	calc activ[h]	max. activ[i]	time max. (min)[j]	$t_{1/2}$[k]
1	**Ni1**	Me/H/H	80	2000	36	5	30		2.00	832	800	1220	4	23
2	**Ni1**	Me/H/H	80	1500	22	5	30		0.84	572	524	944	5	13
3	**Ni1**	Me/H/H	80	1000	21	5	30		0.78	556	652	1080	4	15
4	**Ni1**	Me/H/H	80	500	25	5	30		0.67	404	456	812	6	15
5	**Ni1**	Me/H/H	80	100	26	5	30		0.58	336	336	540	5	n.d.[m]
6	**Ni2**	H/H/H	100	2000	17	5	30	40	2.15	760	984	2196	5	8
7	**Ni2**	H/H/H	80	1000	62	5	30		3.00	724	460	1028	5	32
8	**Ni2**	H/H/H	100	750	14	5	30	39	3.10	1328	1420	1980	3	14
9	**Ni2**	H/H/H	100	250	19	5	30	37	2.65	836	812	1280	3	11
10	**Ni2**	H/H/H	100	50	14	5	30	34	1.72	736	872	1092	6	32
11	**Ni2**	H/H/H	80	100[l]	120	5	30		0.48	60	184	616	10	n.d.[m]
12	**Ni2**	H/H/H	80	10[l]	30	5	30		0.00	0	0	0		
13	**Ni5**	H/NO_2/H	80	2000		5	30	32	0.00	0	792	876	9	n.d.[m]
14	**Ni5**	H/NO_2/H	80	1000	23	5	30	32	0.00	0	168	244	4	25
15	**Ni5**	H/NO_2/H	80	250	19	5	30	31	0.00	0	20	132	2	n.d.[m]
16	**Ni6**	H/OMe/H	100	2000	21	5	30	33	0.81	232	452	792	3	13
17	**Ni6**	H/OMe/H	100	1000	22	5	30	35	1.30	356	340	976	3	17
18	**Ni6**	H/OMe/H	100	50	29	5	30	33	2.00	476	424	1572	4	30
19	**Ni3**	Benz/H/H	80	1000	109	5	30		1.00	136	424	668	3	>50
20	**Ni4**	Ph/H/H	100	75	27	5	30	31	0.30	68	72	472	1	2
21	**Ni4**	Ph/H/H	100	50	14	5	30	40	4.20	1800	1472	2472	5	4
22	**Ni4**	Ph/H/H	100	50	20	5	30	36	2.20	660	588	1100	6	7
23	**Ni4**	Ph/H/H	100	50	26	5	30	40	3.50	808	720	2028	4	10
24	**Ni4**	Ph/H/H	100	50	30	3	30	31	0.04	8	30	60	9	n.d.[m]
25	**Ni4**	Ph/H/H	100	50	7	7	30	53	3.60	3084	2412	5760	2	1[n]
26	**Ni4**	Ph/H/H	100	50	24	5	50	51	0.30	76	28	152	4	8
27	**Ni4**	Ph/H/H	100	50	12	5	14	36	5.4	2700	1624	3772	11	n.d.[m]

[a] Solvent, toluene. [b] Ligand substitution pattern, see Chart2. [c] Experiments with [Ni] = 80 μM carried out in 50 mL (4 μmol) and [Ni] = 100 μM, in 100 mL (10 μmol). [d] Co-catalyst = MMAO unless otherwise stated. [e] Temperature of the external bath. [f] Maximum internal temperature recorded in the experiment. [g] Average productivity from PE weight (kg PE/mol Ni·h). [h] Average activity from ethylene consumption (kg /mol Ni·h). [i] Maximum instantaneous activity recorded in the experiment. [j] Time (min) at the maximum activity. [k] Catalyst half-life, estimated from the activity decay rate. [l] DEAC co-catalyst. [m] No suitable exponential decay curve observed. [n] Approximate value.

Table 3. Polymer and Oligomer Characterization Data

	exptl conditions						polymer data											
							GC	GPC			Branches (^{13}C NMR).						DSC	
entry	cat. no.	R/Z/R′[b]	[Ni] μM[c]	[Ni]/[Al][d]	press (bar)	ext temp (°C)	Flory-Schulz α	Mn 10^{-3}	M_w 10^{-3}	PDI	Me/10^3C	Et/10^3C	Bu/10^3C	Pen10^3C	Hex+/10^3C	MeT/10^3C	T_m	% cryst
1	**Ni1**	H/H/Me	8	2000	5	30					53.9	7.6	1.5	3.0	15.0	80.9	53	3
2	**Ni1**	H/H/Me	8	1500	5	30					57.2	5.6	1.6	3.5	15.2	83.1	55	6
3	**Ni1**	H/H/Me	8	1000	5	30		1.85	3.05	1.65	59.8	6.1	1.7	4.4	14.9	87.0		
4	**Ni1**	H/H/Me	8	100	5	30					58.9	6.6	1.9	4.5	16.4	88.0		
8	**Ni2**	H/H/H	8	2000	11	30	0.81	2[a]										
9	**Ni2**	H/H/H	8	750	11	30	0.85	1.01	1.75	1.74	35.9	5.4	1.8	6.2	16.2	64.5	57	31
10	**Ni2**	H/H/H	8	250	11	30	0.87	1.35	2.22	1.64	31.1	4.6	1.2	5.5	12.4	55.0	57	38
11	**Ni2**	H/H/H	8	50	11	30	0.89	1.49	2.36	1.58	29.3	3.8	1.1	4.9	11.8	51.0	58	46
17	**Ni6**	H/OMe/H	10	2000	5	30		2.28	2.63	1.15	6.2	8.2	2.4	5.5	13.7	36.0		
18	**Ni6**	H/OMe/H	10	1000	5	30	0.92	2.25	2.80	1.24	43.3	5.0	1.7	6.8	13.5	70.2		
19	**Ni6**	H/OMe/H	10	250	5	30	0.91	2.21	2.65	1.20	41.1	5.5	1.6	6.2	13.5	68.0		
20	**Ni6**	H/OMe/H	10	50	5	30		2.07	2.42	1.17	45.1	7.2	2.1	7.1	14.9	76.4		
21	**Ni4**	Ph/H/H	10	75	5	30		21.79	92.35	4.24[b]	21.9	1.9	0.7	0.9	2.5	27.9	107	45
22	**Ni4**	Ph/H/H	10	50	5	30		27.10	77.00	2.84	21.4	3.1	0.6	0.7	2.4	28.3	106	42
23	**Ni4**	Ph/H/H	10	50	5	30		34.06	90.91	2.67	23.2	2.4	0.8	0.9	2.2	29.3	129	44
24	**Ni4**	Ph/H/H	10	40	3	30		6.52	68.61	10.5[c]	21.2	2.5	0.4	0.7	3.7	28.5		
25	**Ni4**	Ph/H/H	10	50	7	30		20.16	57.21	2.84	23.0	2.9	0.6	0.6	3.2	30.2	103	39
26	**Ni4**	Ph/H/H	10	50	5	50		16.62	45.5	2.74	25.2	2.4	0.8	0.7	4.0	33.2	98	35
27	**Ni4**	Ph/H/H	10	50	5	14		76.99	382.3	4.97[d]	13.9	1.2	0.7	0.7	1.1	17.5	130	56

[a] Soluble fraction. [b] Ligand substitution pattern, see Chart2. [c] Experiments with [Ni] = 8 μM carried out in 50 mL (4 μmol) and [Ni] = 10 μM, in 100 mL (10 μmol). [d] From ^{13}C NMR.

ethylene consumption, but no solid or liquid products could be isolated on workup. Standard GC analysis showed the absence of significant amounts of oligomers heavier than C_6,; therefore DEAC causes a shift in the activity from polymerization to dimerization or trimerization, which suggests a profound alteration of the catalyst structure.

Comparison of **Ni2** with the pyridine-substituted catalysts **Ni5** (Z = NO_2) and **Ni6** (Z = OMe) provides some information on the influence of electronic effects on the catalytic performance of the PymNox catalysts. The catalytic properties of compound **Ni6** are not too different from those of **Ni1** and **Ni2**, but the former gives rise to a somewhat less productive catalyst than those originated from the latter two. The lower activity maxima and smaller exotherms recorded for **Ni6** confirm that the introduction of the methoxy group gives rise to an intrinsically less active catalyst. This system is rather sensitive to the MMAO activator, but at low Al/Ni ratios (≈50), it is remarkably stable, with an apparent half-life of 30 min. In spite of the low co-catalyst load, the precatalyst is rapidly activated, which contributes decisively to maintain a relatively good activity average.

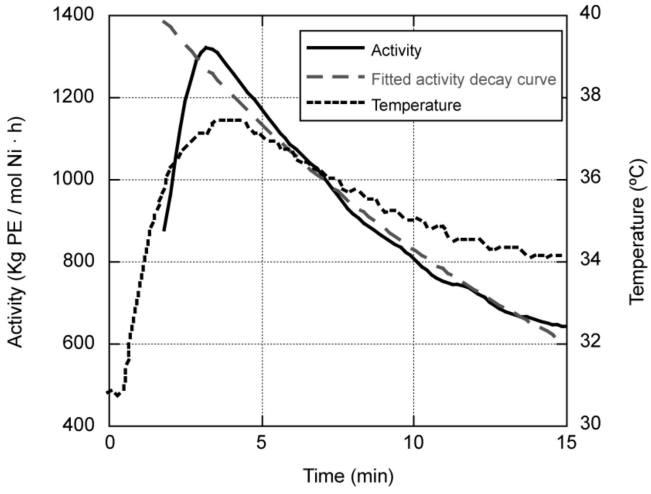

Figure 3. Typical activity and temperature profile for an ethylene polymerization experiment (entry 9, Table 2). Instantaneous activities have been calculated from ethylene uptake data.

It is possible that the interaction of the MeO group with the Lewis acidic Al centers is responsible for the co-catalyst sensitivity observed in this system.

Complex **Ni6** affords significantly heavier ($M_w \approx 2700$) and slightly more branched polyethylenes than **Ni2**, also with a low polydispersity (PDI) ratio (entries 17−20, Table 3). As compared to the latter, the polymer obtained with **Ni6** displays higher molecular weight, in line with the even flatter Flory−Schulz distribution ($\alpha \approx 0.9$) of the soluble oligomeric fraction. Similar electronic effects have been observed in palladium α-diimine system.[26] Likewise, it would be expected that compound **Ni5**, which exhibits a strongly electron-withdrawing NO_2 group in the pyridine ring, should produce lower molecular weight products. Indeed, activation of **Ni5** with MMAO exclusively affords light, volatile oligomers (C4, C6), as observed in the **Ni2**/DEAC system. As already mentioned, ligand **5** appears to be the weakest in the series, and the dramatic selectivity shift observed for the **Ni5** system is likely to be due to some fundamental alteration of its nature (as previously suggested for the **Ni2**/DEAC system), rather than to selectivity modulation by the electron-withdrawing group. Somewhat surprisingly, the activity profiles recorded with both oligomerization catalysts shows that these are long-lived systems.

The influence of substituent groups next to nitrogen in the pyridine ring was explored with compounds **Ni3** and **Ni4**. As already mentioned, Grubbs' salicylaldiminate complexes benefit from this kind of substitution, which provides the most active catalysts and higher molecular weight polymers. Compound **Ni3** is disappointing on this regard, displaying a very low activity level. Only by resorting to long polymerization times can a significant amount of polymer be isolated. The activity profile recorded in a 109 min run (entry 19, Table 2) shows little or no catalyst decay, indicating that, in spite of its low catalytic activity, this is a very stable catalyst. On the contrary, complex **Ni4** shows the expected positive influence of the 6-phenyl substituent, achieving very high activity levels (up to 1800 kg PE/mol Ni·h at 5 bar ethylene pressure) and producing medium to high molecular weight polyethylene with a low level of branching and narrow molecular weight distributions ($M_w = (70-90) \times 10^3$, PDI 2.7−2.8). The DSC data for these products (T_m and crystallinity degree) are typical for LLDPE. A drawback of this catalyst is its low tolerance to the activator agent. Negligible activities were recorded when Al/Ni ratios above 75 are used (entry 20, Table 2). Activity curves are characteristic, featuring high maxima and strong exotherms, followed by rapid decay, indicating that the catalyst is intrinsically very active, but relatively short lived under the selected experimental conditions. The need to initiate the reaction with very small amounts of cocatalyst and the rather limited catalyst stability lead to low experimental reproducibility (compare entries 21−23 in Table 2), but on average this complex gives rise to higher productivities than any of the remaining catalysts.

In order to improve the behavior of the **Ni4**-based catalytst, we studied the influence of temperature and pressure. Increasing the initial reaction temperature to 50 °C nearly causes the shutdown of the catalytic activity (entry 26, Table 2) and affords lower molecular weight polymer (entry 26, Table 3). The same temperature effects are often observed with late transition metal catalysts and are usually attributed to the increase of the catalyst decay rate.[27,28] The activity record for this experiment displays a typical profile with a low maximum (just 150 kg/mol Ni·h), but catalyst decay does not appear to be substantially faster than in the 30 °C experiment. In contrast, this catalyst attains its maximum activity level when activation is started at 14 °C (entry 27, Table 2). In this experiment, catalytic activity is observed to gradually increase over time, with the maximum level being reached at the end of the experiment. This is consistent with slow but efficient catalyst activation, together with inappreciable decay. The parallel rise of the reactor temperature (from 14 to 32 °C) complicates the measure of the monomer consumption due to the pressure compensation effect, and the weight of the polymer is actually significantly larger than that calculated from the ethylene consumption data. The inhomogeneous temperature conditions during the experiment are also reflected by the broad polymodal polymer molecular weight distribution that displays two main peaks at 103.000 and 800.000 amu.

Entries 23, 24, and 25 (Table 2) illustrate the dramatic influence of the ethylene pressure on the catalytic activity of the **Ni4** catalyst. On going from 3 to 7 bar, the average productivity experiences a 100-fold increase. This is clearly a nonlinear effect and cannot be uniquely related to the variation of monomer concentration in the solution. In fact, rapid catalyst deactivation was observed at both the highest and lowest pressures, suggesting that the interplay of different factors, such as the dependency of the catalyst stability on the monomer concentration, the efficiency of the activation process, and the reactor temperature, leads to a very complicated situation. At 7 bar, very high catalytic activities are rapidly achieved. The causes of the rapid catalyst decay in this experiment are unclear. Thermal deactivation (the reactor temperature rises above 53 °C) or encapsulation of the catalyst in the polymer and precipitation are possible explanations.

Although the polymer produced at the lower pressure has a broad, polymodal distribution (possibly due to the irregular catalyst performance), neither the molecular weight nor the number and type of branches appear to be significantly altered by pressure between 3 and 7 bar. This suggests that monomer concentration has little effect on the chain propagation/walking rate balance, in contrast with the observations in the α-diimine

(26) Popeney, C.; Guan, Z. *Organometallics* **2005**, *24*, 1145.

(27) Gates, D. P.; Svejda, S. A.; Oñate, E.; Killian, C. M.; Johnson, L. K.; White, P. S.; Brookhart, M. *Macromolecules* **2000**, *33*, 2320.

(28) Britovsek, G. J. P.; Bruce, M.; Gibson, V. C.; Kimberley, B. S.; Maddox, P. J.; Mastroianni, S.; McTavish, S. J.; Redshaw, C.; Solan, G. A.; Strömberg, S.; White, A. J. P.; Williams, D. J. *J. Am. Chem. Soc.* **1999**, *121*, 8728.

nickel system.[27] However our data are clearly insufficient on this regard, and more experiments are necessary to clarify this point.

As a final consideration in this section, it is interesting to compare the catalytic features of the cationic PymNox and neutral salicylaldiminate system. The exact salicylaldiminate counterparts of the PymNox ligands **2**, **4**, **5**, and **6** have been used by Grubbs in polymerization catalysis.[7] It must be considered that the different experimental conditions (particularly the higher pressures employed in the studies on the neutral system) make difficult or impossible an accurate comparison between the two systems. In addition, since Grubbs' catalyst precursors contain a reactive Ni−C bond and a labile PPh_3 ligand, they can behave as single-component catalysts. However, activation of the salicylaldiminato complexes with suitable phosphine scavengers ($Ni(cod)_2$ or $B(C_6F)_3$) renders the neutral catalysts more akin to those formed by the halide PymNox complexes/alumoxane combination.[7a] Under these conditions the neutral catalysts are approximately 1 order of magnitude less active than the cationic ones, and the difference is even more marked if the pressure effects are included in the activity units. At the same time, polymers produced by the cationic system have comparable molecular weights and branching degree. For example, upon activation with $Ni(cod)_2$, the neutral salicylaldiminato analogue of **Ni2** displays a modest activity of just 40 kg/mol Ni·h and produces low molecular weight PE ($M_w = 4000$) at 7 bar (**Ni2**: 1300 kg/mol Ni·h and $M_w \approx 2000$ at 5 bar). However, there are evident analogies in the influence of catalyst structure. For example, the introduction of aryl substituents at position 6 in the pyridine ring is a crucial factor in both systems, improving both activity and product molecular weight. In the neutral system, phenyl substitution at position 6 causes a 4-fold increase in activity with respect to the unsubstituted catalyst and produces PE with $M_w = 23\,500$ (at the same pressure, 7 bar, **Ni4** has an activity of ca. 3000 kg/mol Ni·h, and the M_w is 57000). The presence of an electron-donor methoxy substituent in the pyridine ring also has a similar impact in the two catalytic systems, leading to a moderate increase of the molecular weight and some decrease of activity. The effect of the electron-withdrawing NO_2 group marks one of the most obvious differences between the salycylaldiminato and PymNox systems: while it leads to high molecular weight polyethylene in the neutral catalysts (with broad PDI), the cationic PymNox counterpart (**Ni5**) affords only light oligomers. The striking difference between these two catalysts supports our interpretation that the ethylene oligomerization activity by **Ni5** is actually due to some kind of catalyst decomposition or alteration. Although significantly less active, the salicylaldiminato catalysts appear to benefit from better thermal stability than PymNox catalysts on a general basis. This is particularly true when the former are allowed to act as single-component catalysts in the absence of any activating agent,[7b] although the catalytic activities are still lower under such conditions.

Copolymerization of Ethylene and Methyl Acrylate. An important objective of this work is to investigate the ability of PymNox catalysts to copolymerize ethylene with methyl acrylate. Systematic copolymerization tests have been performed for each of the nickel catalysts under optimum conditions found for ethylene homopolymerization. In these experiments, the methyl acrylate concentration was set to 0.24 M, while the ethylene concentration under these conditions was ca. 0.5 M.[29] In order to avoid any interference of the co-monomer in the catalyst activation process, methyl acrylate (1 mL) was introduced ca. 1−3 min after triggering the polymerization with MMAO. For most of the catalysts, this procedure results in complete activity quench. The exception is catalyst **Ni1**, which produces a small amount of polymer.

The ethylene−methyl acrylate copolymer is considerably more soluble than polyethylene, hampering its quantitative isolation of small amounts, and this made it difficult to estimate the catalytic activity for short reaction times. However, the yield of isolated product in the 3 h run, ca. 650 mg, indicates an average activity of ca. 20 kg/mol·h. In order to maximize the amount of polymer recovered, the product was simply washed with aqueous HCl to remove any traces of aluminum. In favorable cases, the homogeneity of the product was checked by re-precipitation from a dichloromethane solution with tetrahydrofuran (see Experimental Section). We have not carried out full characterization of the products, but their spectroscopic features and higher solubility strongly support that these are ethylene−methyl acrylate copolymers. Thus, they display a characteristic IR absorption band at 1716 cm^{-1} and their ^1H NMR spectra show a characteristic signal at δ 3.67 ppm, due to the methoxycarbonyl group. A two-dimensional DOSY (Diffusion Ordered SpectroscopY; see Supporting Information) experiment showed that the methoxycarbonyl group displays the same diffusion coefficient as the bulk polyethylene fragments, and very likely they belong to a true copolymer and not to a mixture of homopolymers. From the relative intensity of the two groups of signals, a methyl acrylate incorporation of ca. 0.7 mol % can be deduced. The overall intensity of the vinyl groups (>80% internal) allows an estimation of M_n of about 1900, very similar to the M_n value (GPC) of the homopolymer produced by the same catalyst. Direct observation of the ^{13}C resonances belonging to the inserted acrylate units other than those of the O*Me* group (δ 51.9 ppm) and the carboxylate carbon (δ 175.0 ppm) is difficult, due to the low acrylate content of the polymer and the wealth of signals in the 10−40 ppm region, corresponding to the branched polyethylene framework. However, the 2D long-range C−H heterocorrelation experiment (HMBC) display several cross-peaks that related the ^{13}C carbonyl signal (δ 175 ppm) to the ^1H resonances of the neighboring groups. Besides an intense correlation with the methoxycarbonyl group, another four cross-peaks can be located at δ 2.3, 2.0, 1.7, and 1.6 ppm. These find correspondences with ^{13}C spectral zones in the one-bond HSQC heterocorrelation experiment at δ 41.4, 39.7, 34.4, and 30.1 ppm, respectively. The signal couples 2.3 (H)/41.4 (C) ppm and 1.6 (H)/30.1 (C) are not very different from those observed by Drent for the ethylene−methyl acrylate copolymer obtained with palladium phosphinosulfonato catalysts[9a] (2.28 (H)/45.7 (C) (>C*H*CO_2Me); 1.56 (H), 32.4 (...C*H*$_2$CH(CO_2Me)*CH*$_2$...)) and attributed to methyl acrylate units directly inserted into the polyethylene chain. On the other hand, the pairs 2.0 (H)/39.7 (C) and 1.7 (H)/34.4 (C) compare well with the signals observed for the >*CH*-*CH*$_2$$CO_2$Me unit in methyl 3-ethylhexanoate or methyl 3-ethyloctanoate (CH_2: 2.15 (H)/38.5 (C); CH: 1.73 (H), 36.1 (C) ppm)[30] and therefore suggest the presence of short CH_2CO_2Me branches. However, longer branches ending in carboxylate groups, similar to those obtained with the α-diimine palladium catalyst system,[3a] are apparently absent in this copolymer, since the characteristic cross-peaks for the terminal *CH*$_2$$CO_2$Me methylene groups (2.2 (H), 34.2 (C) in methyl undecanoate) could not be located.

(29) Lee, L.; Ou, H.; Hsu, H. *Fluid Phase Equilibria* **2005**, *231*, 221.

(30) López, F.; Harutyunyan, S. R.; Meetsma, A.; Minnaard, A. J.; Feringa, B. L. *Angew Chem., Int. Ed.* **2005**, *117*, 2812.

Conclusion

2-Iminopyridine *N*-oxides (PymNox) are promising ligands for applications in catalysis. One of the advantages of these ligands is that their synthesis is considerably facilitated by the rich chemistry of heteroaromatic *N*-oxides. They form stable complexes with nickel and palladium, the former becoming active catalysts for the ethylene polymerization or oligomerization on treatment with alumoxanes or DEAC. This demonstrates that the electrically neutral *N*-oxide functionality successfully substitutes anionic oxygen donor groups widespread in olefin polymerization or oligomerization catalysts, e.g., the SHOP-type or salicylaldiminate catalysts, giving rise to functional cationic counterparts. PymNox nickel catalysts are more active than their neutral salicylaldiminato-based analogues, but otherwise the two systems display many analogies: they give rise to similar polymers in terms of both molecular weights and branching degree, and display similar trends in the influence of ligand structure on catalyst performance. Thus, electronic effects modulate catalytic activity, with electron-donor groups leading to somewhat decreased activities. More importantly, substitution at position 6 in the aromatic ring with aromatic groups leads to dramatic increases in both activity and polymer molecular weight. Similarly to salicylaldiminate catalysts, 2-aldiminopyrdine *N*-oxide catalysts are not compatible with methyl acrylate.[3d] However, the ketimino derivative **Ni1** copolymerizes this comonomer with ethylene. NMR analysis suggests that the resulting ethylene−methyl acrylate copolymer displays both directly inserted acrylate units and short CH_2CO_2Me branches. Further research directed to the optimization of the PymNox ligands and catalysts for olefin polymerization and copolymerization reactions are currently being carried out in our laboratories.

Experimental Section

All the complexes' synthesis and catalyst preparations were carried out under a dry nitrogen atmosphere by conventional Schlenk techniques. Solvents were rigorously dried by refluxing over sodium benzophenone (toluene, hexane, diethyl ether, tetrahydrofuran) or calcium hydride (CH_2Cl_2) and freshly distilled prior to use. Deuterated solvents (Aldrich) were dried over CaH_2 (CD_2Cl_2, $CDCl_3$) or sodium benzophenone (C_6D_6) and then distilled. Pyridine derivatives and other organic reagents were purchased from Aldrich and used without further purification. $NiCl_2$(dme) was synthesized as reported in the literature.[31] MMAO (1.8 M in heptane) was purchased from Akzo-Nobel and used without further purification. IR spectra were recorded on a Bruker Vector 22, and UV−vis on a Perkin-Elmer model Lambda-12. NMR spectra were obtained on Bruker Avance DRX 500 (500 MHz), Bruker Avance DRX 400 (400 MHz), and Bruker Avance 300 (300 MHz) spectrometers. The ^{1}H and ^{13}C{^{1}H} resonances of the solvent were used as internal standard, but the chemical shifts (ppm) are reported with respect to TMS. Elemental analyses were performed by the Micro-analytical Service of the Instituto de Investigaciones Químicas. Molecular weights of the polymers were determined by gel permeation chromatography employing universal calibration in a Waters 150c instrument with differential refractive index (DRI) detector and a Viscotek 150R DV detector.

Ligand Synthesis. General Procedure A: *N*-Oxidation of 2-Acetylpyridine. 2-Acetylpyridine *N*-Oxide. A mixture of 2-acetylpyridine (20 mmol) and mCPBA (70 mmol) in $CHCl_3$ (25 mL) was refluxed for 4 h. The solvent was removed under vacuum, and the resulting product was purified by flash chromatography (TLC (SiO_2, CH_2Cl_2/acetone, 1:1) R_f = 1 organic residues, 0.8 mCPBA, 0.2 product) using first CH_2Cl_2 as eluent to remove the excess mCPBA as the first fraction and then acetone to extract the product in the second fraction. ^{1}H NMR (400 MHz, $CDCl_3$, 298 K): δ 8.17 (d, $^3J_{HH}$ = 6.8Hz, 1H, Ar meta), 7.67 (d, $^3J_{HH}$ = 10Hz, 1H, Ar ortho 3), 7.34 (t, 1H, Ar para), 7.30 (t, 1H, Ar ortho 5), 2.77 (s, 3H, Me). Anal. Calcd (%) for $C_7H_7NO_2$ (137.14 g/mol): C 61.31; H 5.14; N 10.21. Found: C 60.98; H 5.15; N 10.54.

2-[*N*′-(2,6-Diisopropylphenyl)acetaldimino]pyridine *N*-Oxide (1). A mixture of 2-acetylpyridine *N*-oxide (1.37g, 10 mmol) and 2,6-diisopropylaniline (2.83 mL, 15 mmol) was dissolved in dry toluene (20 mL) and refluxed for 2 h in a Dean-Stark apparatus. The solvent was removed under vacuum, and the resulting oil was purified by flash chromatography with $CHCl_3$ to extract the excess of aniline and with acetone to extract the product. After removing the solvent under vacuum 2.5 g (89%) of the product was afforded as a brown oil. Mp = 77 °C. ^{1}H NMR (500 MHz, $CDCl_3$, 298 K): δ 8.22 (d, $^3J_{HH}$ = 7.5 Hz, 1H,CH Py 6); 7.62 (d, $^3J_{HH}$ = 9.6 Hz, 1H, CH Py 3); 7.34 (t, 1H, CH Py 4); 7.32 (t, 1H, CH Py 5); 7.15 (d, $^3J_{HH}$ = 7,5 Hz, 2H, m-CH(Ar)); 7.10 (t, $^3J_{HH}$ = 7.5 Hz, 1H, p-CH(Ar)); 2.87 (m, 2H, CH iPr); 2.18 (s, 3H, CH_3); 1.21 (d, $^3J_{HH}$ = 7.15 Hz, 6H, CH_3 (iPr)); 1.15 (d, $^3J_{HH}$ = 7.15 Hz, 6H, CH_3 (iPr)). ^{13}C{^{1}H} NMR (75 MHz, $CDCl_3$, 298 K): δ 165.3 (1C, *C*=N); 149.9 (1C, Cq Py 2); 144.9 (1C, C_{ipso} Ar); 140.5 (1C, CH Py 6); 136.4 (2C, Cq-iPr); 126.5 (1C, CH Py 5); 126.5 (1C, CH Py 4); 126.3 (1C, CH Py 3); 124.6 (1C, p-CH Ar); 123.5 (2C, o-CH Ar); 28.4 (2C, CH (iPr)); 23.8 (2C, CH_3 (iPr)); 23.2 (2C, CH_3 (iPr)); 20.2 (1C, CH_3 (Py)). IR (Nujol, cm^{-1}): 1635.7 ν(C=N); 1254.5 ν(N−O). UV/vis (CH_2Cl_2, $c = 10^{-5}$ M (ϵ, 10^5 mol^{-1}·L·cm^{-1}): 363 (0.337); 290 (1.175); 248 (2.93). MS (ESI, MeOH) *m/z*: 296.17 [M$^+$]. Anal. Calcd (%) for $C_{19}H_{24}N_2O$ (296.41 g/mol): C 76.99; H 8.16; N 9.45. Found: C 76.29; H 8.10; N 9.24.

General Procedure B: 2-Pyridinecarbaldehyde *N*-Oxide. Adapted from the literature.[19,21] A mixture of picoline *N*-oxide (5.45 g, 50 mmol) and selenium dioxide (5.54 g, 50 mmol) in pyridine (25 ml) was heated under reflux for 5 h. The solid material was filtered off, the filtrate was concentrated in vacuo, and the residual oil was extracted four times with hot toluene (50 ml). TLC (silica, acetone/ether, 2:1): R_f = 0.4 product; 0.08 picoline *N*-oxide. Flash chromatography with acetone/ether (2:1) afforded the product as the first fraction. The solvent was removed in vacuo, and the product was obtained as a yellow solid (5.16 g, 83%). ^{1}H NMR (500 MHz, $CDCl_3$, 298 K): δ 10.61 (s, 1H, C<u>H</u>O); 8.19 (d, $^3J_{HH}$ = 6.5Hz, 1H, C<u>H</u> Py 2); 7.80 (d, $^3J_{HH}$ = 7Hz, 1H, CH Py 5); 7.43 (t, $^3J_{HH}$ = 6.5 Hz, 1H, CH Py 3); 7.30 (t, $^3J_{HH}$ = 7Hz, 1H, CH Py 4). Anal. Calcd (%) for $C_6H_5NO_2$ (123.10 g/mol): C 58.54; H 4.09; N 11.38. Found: C 58.06; H 4.11; N 11.25.

General Procedure C: Aniline Condensation. 2[-(*N*′-2,6-Diisopropylphenyl)carbaldimino]pyridine *N*-Oxide (2). A mixture of 2-carboxyaldehyde pyridine *N*-oxide (5.16 g, 42 mmol), 2,6-diisopropylaniline (8 mL, 42 mmol), and a catalytic amount of acetic acid in methanol (200 mL) was refluxed for 4 h. The mixture was concentrated under vaccuum and allowed to crystallize upon cooling in hexane. The product was filtered off and recovered as a yellow crystalline solid (9.43 g, 79% at this step, 66% for the whole synthesis). Mp = 130.4 °C. ^{1}H NMR (400 MHz; $CDCl_3$; 298 K): δ 8.89 (s, 1H, CH=N); 8.23 (d, $^3J_{HH}$ = 4Hz, 1H, CH Py 2); 8.18 (d, $^3J_{HH}$ = 7Hz, 1H, CH Py 5); 7.35 (m, 2H, CH Py 3 and 4); 7.13 (m, 3H, CH Ar); 2.91 (m, 2H, CH iPr); 1.16 (d, $^3J_{HH}$ = 7Hz, 12H, CH3 iPr). ^{13}C{^{1}H} NMR (75 MHz, $CDCl_3$, 298 K): δ 155.4 (1C, CH=N); 148.6 (1C, C_q-NO); 145.8 (C_q-N=C); 140.3 (1C, CH 6 py); 137.5 (2C, C_q-iPr); 127.6 (1C, CH 5 Py); 125.8 (1C, CH p-Ar); 125.2 (1C, CH 4 Py); 124.8 (1C, CH 3 Py); 123.4 (2C, CH o-Ar); 28.2 (2C, $CH(CH_3)_2$); 23.7 (4C, $CH(CH_3)_2$). IR (Nujol): ν 1628 cm^{-1} (C=N); 1603 (C=N); 1251 (N−O). UV/vis (CH_2Cl_2, 10^{-4} M, λ = nm, $\epsilon = 10^{-4}$ mol^{-1}·L·cm^{-1}): 363 (0.337); 290 (1.175); 248 (2.93). MS (ESI; MeOH) *m/z*: 321 [M + K]$^+$; 305 [M + Na]$^+$;

(31) (a) Cotton, F. A. *Inorg. Synth.* **1971**, *13*, 162. (b) Cotton, F. A. *Inorg. Synth.* **1971**, *13*, 47.

283 $[M + H]^+$. Anal. Calcd (%) for $C_{18}H_{22}N_2O$ (282.38 g/mol): C 76.56; H 7.85; N 9.92. Found: C 75.94; H 7.95; N 9.81.

Quinaldine *N*-Oxide. The general procedure A using quinaldine (1.35 mL; 10 mmol). TLC (SiO_2, ether/petroleum ether, 1:1). The product crystallizes in ether upon cooling, affording a pale brown solid (1.4 g, 90%). ^{1}H NMR (400 MHz; $CDCl_3$; 298 K): δ 8.74 (d, 1H, CH 3); 7.79 (d, 1H, CH 6); 7.70 (t, 1H, CH 8); 7.64 (d, 1H, CH 9); 7.55 (t, 1H, CH 7); 7.29 (d, 1H, CH 4); 2.70 (s, 3H, CH_3). Anal. Calcd (%) for $C_{10}H_9NO$ (159.18 g/mol): C 75.45; H 5.70; N 8.80. Found: C 74.87; H 5.64; N 8.71.

Quinoleine-2-carbaldehyde *N*-Oxide. The general procedure B using quinaldine *N*-oxide (1.4 g, 9 mmol). TLC (silica, ether): $R_f = 0.6$, product; 0, quinaldine *N*-oxide. Flash chromatography with ether afforded the product as a yellow solid (1.16 g, 74% at this step, 63.5% starting from quinaldine). ^{1}H NMR (300 MHz; $CDCl_3$; 298 K): δ 10.83 (s, 1H, CHO); 8.76 (d, 1H, CH 3); 7.88 (d, 1H, CH), 7.77 (m, 4H, CH). Anal. Calcd (%) for $C_{10}H_7NO_2$ (173.16 g/mol): C 69.36; H 4.07; N 8.09. Found: C 70.10; H 4.08; N 8.15.

2-(*N*′-2,6-Diisopropylphenylimino)methyl]carbaldiminoquinoleine *N*-Oxide (5). The general procedure C using 2-carboxyaldehyde quinoline *N*-oxide (1.16 g, 6.35 mmol). The product was recovered as a yellow crystalline solid after filtration (1.9 g, 90% in this step, 57% for the whole synthesis). Mp = 85.8 °C. ^{1}H NMR (400 MHz; $CDCl_3$; 298 K): δ 9.13 (s, 1H, CH═N); 8.77 (d, $^3J_{HH}$ = 8.8Hz, 1H, CH 3); 8.22 (d, $^3J_{HH}$ = 8.8Hz, 1H, CH 4); 7.89 (d, $^3J_{HH}$ = 8Hz, 1H, CH 6); 7.78 (m, 2H, CH 8 and 9); 7.70 (t, $^3J_{HH}$ = 8Hz, 1H, CH 7,); 7.16 (m, 3H, CH Ar); 2.96 (m, 2H, $CH(CH_3)_2$); 1.18 (d, $^3J_{HH}$ = 6.8Hz, 12H, $CH(CH_3)_2$). ^{13}C{^{1}H} NMR (75 MHz; $CDCl_3$; 298 K): δ 156.1 (1C, CH═N); 148.9 (1C, Cq Py 2); 142.4 (1C, C_{ipso} Ar); 142.2 (1C, Cq 10 quin.); 137.6 (2C, Cq-iPr); 131.3 (1C, Cq 5 quin.); 130.9 (1C, CH 8 quin.); 130.0 (1C, CH 4 quin.); 128.6 (1C, CH 3 quin.); 125.7 (1C, CH 7 quin.); 125.3 (1C, CH p-Ar); 123.4 (2C, CH o-Ar); 120.2 (1C, CH 9 quin.); 119.7 (1C, CH 6 quin.); 28.3 (2C, $\underline{C}H(CH_3)_2$); 23.8 (4C, $CH(\underline{C}H_3)_2$). IR (Nujol, cm^{-1}): 1726; ν(C═N) 1618,8; ν(N−O) 1230. UV/vis (CH_2Cl_2, 10^{-4} M, λ = nm, $\epsilon = 10^{-4}$ $mol^{-1}\cdot L\cdot cm^{-1}$): 381 (0.423); 325 (0.587); 282 (2.59); 247 (2.33). MS (ESI; MeOH) *m/z*: 355.1 $[M + Na]^+$. Anal. Calcd (%) for $C_{22}H_{24}N_2O$ (332.44 g/mol): C 79.48; H 7.27; N 8.42. Found: C 79.53; H 7.39.

2-Methyl-6-bromopyridine. Adapted from literature.[21] Powdered 2-aminopicoline (5.4 g, 50 mmol) was added in portions to 48% hydrobromic acid (25 mL) at 20 to 30 °C with vigorous stirring. After the entire compound was dissolved, the mixture was cooled at −20°C. To this suspension was added cooled bromine (7.5 mL, 150 mmol) dropwise over 30 min, maintaining the temperature at −20 °C. The resulting paste was stirred for 90 min at this temperature. Then sodium nitrite (10g, 150 mmol) in water (100 mL) was added dropwise. After that the reaction mixture was allowed to warm to 15 °C over 1 h and was stirred for an additional 45 min. The mixture was cooled to −20 °C and treated with cooled aqueous NaOH (33 g, 50 mL of H_2O). During the addition the temperature was kept at −10 °C maximum. The mixture was allowed to warm to room temperature and stirred for 1 h. The mixture was extracted with ethyl acetate, the organic phase was dried with $MgSO_4$, and the solvent was removed in vacuo. The residue was purified by flash chromatography (TLC: SiO_2 ether/hexane, 1:8; $R_f = 0.58$ impurities; 0.29 product) to yield the desired 2-bromopicoline as a brown oil (3.53g, 40%). ^{1}H NMR (300 MHz; $CDCl_3$; 298 K): δ 2.51 (s, 3H, Me); 7.08 (d, $^3J_{HH}$ = 7.5 Hz, 1H, H5); 7.26 (d, $^3J_{HH}$ = 7.5 Hz, 1H, H3); 7.38 (t, $^3J_{HH}$ = 7.5 Hz, 1H, H4). Anal. Calcd (%) for C_6H_6BrN (172.02 g/mol): C 41.89; H 3.52; N 8.14. Found: C 42.01; H 3.65; N 8.15.

2-Methyl-6-phenylpyridine. Adapted from literature.[19] To a mixture of 2-bromo-6-methylpyridine (1.76 g, 10.2 mmol), [Ni(acac)$_2$] (32 mg, 0.13 mmol), and P(^{t}Bu)$_3$ (0.13 mL, 0.13 mmol) in 20 mL of diethyl ether in an ice bath was added phenylmagnesium bromide (7.8 mL, 1 M in diethyl ether) over a period of 10 min. After the solution was heated overnight in a closed ampule under argon, it was hydrolyzed by pouring it into 20 mL of diluted hydrochloric acid. The solution was stirred for 15 min before the organic phase was separated. The aqueous phase was extracted twice (15 mL) with diethyl ether, and the ether was again discarded. The aqueous phase was neutralized by slow addition of Na_2CO_3 until no further CO_2 evolution was observed and a pale yellow precipitate was formed. The basic solution was extracted three times with CH_2Cl_2 (20 mL), and the organic phase was dried over $MgSO_4$. Then the CH_2Cl_2 fraction was evaporated under reduced pressure, yielding a NMR-pure brown oil, which was used directly (1.63 g, 94%). ^{1}H NMR (400 MHz; $CDCl_3$; 298 K): δ 2.65 (s, 3H, py-CH3); 7.09 (d, $^3J_{HH}$ = 7.6 Hz, 1H, py H5); 7.41 (dd, $^3J_{HH}$ = 8.6 Hz, $^4J_{HH}$ = 1.7 Hz, 1H, Ph Hp); 7.46 (d, $^3J_{HH}$ = 7.8 Hz, 1H, py H3); 7.50 (d, $^3J_{HH}$ = 8.6 Hz 2H, Ph Hm); 7.62 (d, $^3J_{HH}$ = 7.8 Hz, 1H, py H4); 7.7 (dd, $^3J_{HH}$ = 8.7 Hz, $^4J_{HH}$ = 1.7 Hz, 2H, Ph Ho). Anal. Calcd (%) for $C_{12}H_{11}N$ (169.22 g/mol): C 85.17; H 6.55; N 8.28. Found: C 84.95; H 6.68; N 8.02.

2-Methyl-6-phenylpyridine *N*-Oxide. The general procedure A using 2-methyl-6-phenylpyridine (1.63g; 9.6 mmol). TLC (SiO_2, ether/petroleum ether, 1:1). The product crystallizes in ether upon cooling, affording a pale yellow solid (1.16 g, 65.5%). ^{1}H NMR (400 MHz; $CDCl_3$; 298 K): δ 2.56 (s, 3H, Me); 7.2 (d, 1H, H3 Py); 7.23 (t, 1H, H4 Py); 7.29 (dd, 1H, H6 Py); 7.24 (t, 1H, Hp Ph); 7.43 (dd, 2H, Hm Ph); 7.76 (dd, 2H, Ho Ph). Anal. Calcd (%) for $C_{12}H_{11}NO$ (185.22 g/mol): C 77.81; H 5.99; N 7.56. Found: C 77.50; H 5.89; N 7.36.

2-Carbaldehyde-6-phenylpyridine *N*-Oxide. The general procedure B using 2-methyl-6-phenylpyridine *N*-oxide (1.16 g, 6.27 mmol). TLC (silica, ether): $R_f = 0.7$ (2-carbaldehyde-6-phenylpyridine *N*-oxide), 0.16 (2-methyl-6-phenylpiridine *N*-oxide). Flash chromatography with ether afforded the product as the first fraction (440 mg, 35%), and with ethyl acetate the starting product was extracted in a second fraction (550 mg). ^{1}H NMR (400 MHz; $CDCl_3$; 298 K): δ 10.67 (s, 1H, HC═N); 7.78 (d, 1H, Py 3); 7.75 (d, 2H, Ph o); 7.59 (d, 1H, Py 5); 7.53 (t, 1H,Py 4); 7.5 (d, 2H, Ph m); 7.35 (t, 1H, Ph p). Anal. Calcd (%) for $C_{12}H_9NO_2$ (199.20 g/mol): C 72.35; H 4.55; N 7.03. Found: C 71.96; H 4.40; N 6.95.

(2-[1-(2,6-Diisopropylphenylimino)methyl]-6-phenyl)pyridine *N*-Oxide (4). The general procedure C using 2-carboxyaldehyde-6-phenylpyridine *N*-oxide (440 mg, 2.2 mmol). The product crystallized upon cooling in hexane and was recovered after filtration as a yellow crystalline solid (709 mg, 90%). Mp = 132.5 °C. ^{1}H NMR (500 MHz; $CDCl_3$; 298° K): δ 1.18 (s, 12H, $CH(CH_3)_2$); 2.96 (m, 2H, $CH(CH_3)_2$); 7.12 (t, $^3J_{HH}$ = 7.5Hz, 1H, Ar-p); 7.16 (d, $^3J_{HH}$ = 7.5Hz, 2H, Ar-m); 7.36 (t, $^3J_{HH}$ = 8Hz, 1H, Py 4); 7.46 (t, 1H, Ph-p); 7.47 (m, 2H, Ph-m); 7.51 (dd, $^3J_{HH}$ = 8Hz, $^4J_{HH}$ = 2Hz, 1H, Py 5); 7.78 (d, $^3J_{HH}$ = 8Hz, 2H, Ph-o); 8.16 (dd, $^3J_{HH}$ = 8Hz, $^4J_{HH}$ = 2Hz, 1H, Py 3); 8.94 (s, 1H, HC═N). ^{13}C{^{1}H} NMR (125 MHz; $CDCl_3$; 298 K): δ 23.5 (4C, $CH(CH_3)_2$); 28.0 (2C, $CH(CH_3)_2$); 123.1 (2C, Ar-m); 123.5 (1C, CH Py 3); 124.8 (1C, CH Ar-p); 124.8 (1C, CH Py 4); 128.4 (2C, CH Ph-o); 128.7 (1C, CH Py 5); 129.4 (2C, CH Ph-m); 129.7 (1C, CH Ph-p); 132.4 (1C, C_{ipso} Ph); 137.3 (2C, Ar C_q-($CH(CH_3)_2$)); 146.2 (1C, Ar C_q-N); 148.4 (1C, Py C_q-CHN); 150.0 (1C, Py C_q-C_6H_5); 156.0 (1C, CH═N). IR (Nujol): ν 1623, 1586, 1321, 1292, 1250, 1234, 1190, 1160. UV/vis (CH_2Cl_2, 10^{-5} M, λ = nm, $\epsilon = 10^{-5}$ $mol^{-1}\cdot L\cdot cm^{-1}$): 369 (0.107); 278 (0.781); 227 (3.17). MS (ESI; MeOH) *m/z*: 359.2 $[M + H]^+$; 381.2 $[M + Na]^+$; 397.2 $[M + K]^+$. Anal. Calcd (%) for $C_{24}H_{26}N_2O$ (358.47 g/mol): C 80.41; H 7.31; N 7.81. Found: C 80.44; H 7.35; N 7.83.

4-Nitro-2-picoline *N*-Oxide. Adaptation from literature.[22] A solution of 2-picoline *N*-oxide (5.45 g, 50 mmol) and KNO_3 (15 g) in concentrated H_2SO_4 (50 mL) was heated for 20 h at 80 °C. The mixture was neutralized by addition of Na_2CO_3 until the compound precipitated. Filtration and recrystallization from CH_2Cl_2

gave 4 g (50%) of the pure product. ^{1}H NMR (300 MHz; $CDCl_3$; 298 K): δ 8.28 (d, $^3J_{HH}$ = 7Hz, 1H, H2); 8.1 (d, $^4J_{HH}$ = 3Hz, 1H, H5); 7.96 (dd, $^4J_{HH}$ = 3Hz; $^3J_{HH}$ = 7Hz, 1H, H3); 2.53 (s, 3H, Me). IR (Nujol): ν 1681 cm^{-1} (C═N); 1610 (C═N); 1286 (N−O). Anal. Calcd (%) for $C_6H_6N_2O_3$ (154.12 g/mol): C 46.76; H 3.92; N 18.18. Found: C 46.78; H 3.83; N 18.58.

4-Nitro-2-carbaldehydepyridine *N*-Oxide. The general procedure B, using 4-nitropicoline *N*-oxide (4 g, 26 mmol). TLC (silica, acetone/ether, 1:3): R_f = 0.7 product; 0.07 picoline *N*-oxide. Flash chromatography with acetone afforded the product as a yellow solid (1.74 g, 40%). ^{1}H NMR (300 MHz; $CDCl_3$; 298 K): δ 10.46 (s, 1H, CHO); 8.58 (s, 1H, H5); 8.28 (d, 1H, H2); 8.11 (d, 1H, H3). Anal. Calcd (%) for $C_6H_4N_2O_4$ (168.10 g/mol): C 42.87; H 2.40; N 16.66. Found: C 42.65; H 2.53; N 16.25.

4-Nitro-2-[*N*′-(2,6-diisopropylphenylimino)carbaldimino]pyridine *N*-Oxide (5). The general procedure C using 4-nitro-2-carboxyaldehyde pyridine *N*-oxide (1.74 g, 10.35 mmol). The product was purified by flash chromatography with CH_2Cl_2/ether/hexane, 1:1:2. TLC: silica (CH_2Cl_2/ether/hexane, 1:1:2) (R_f = 0.89 aniline; 0.46 product; 0.1 picoline *N*-oxide). The product was recovered as a yellow crystalline solid (1.5 g, 45% for the whole synthesis). Mp = 123.1 °C. ^{1}H NMR (300 MHz; $CDCl_3$; 298 K): δ 8.91 (d, $^4J_{HH}$ = 7Hz 1H, H3); 8.77 (s, 1H, CHN); 8.28 (d, $^3J_{HH}$ = 7.2Hz, 1H, H6); 8.16 (dd, $^3J_{HH}$ = 7.2Hz, $^4J_{HH}$ = 3.4Hz, 1H, H5); 2.86 (m, 2H, C*H*(CH$_3$)$_2$); 1.17 (s, 6H, CH(*CH*$_3$)$_2$); 1.16 (s, 6H, CH(*CH*$_3$)$_2$). ^{13}C{^{1}H} NMR (75 MHz; $CDCl_3$; 298 K): δ 153.6 (1C, CH═N); 148.0 (1C$_q$, C$_2$−CHN); 146.8 (1C$_q$, C$_{ipso}$ Ar); 142.5 (1C$_q$, C$_4$−NO$_2$); 141.5 (1C. CH Py 5); 137.5 (2C$_q$, C-CH(CH$_3$)$_2$); 125.8 (1C, CH Ar p); 123.5 (2C, CH Ar m); 121.3 (1C, CH Py 3); 119.4 (1C, CH Py 6); 28.3 (2C, CH(CH$_3$)$_2$); 23.8 (4C, CH(CH$_3$)$_2$). IR (Nujol): ν = cm^{-1} 1630 (C═N); 1608 (C═N); 1343 (NO$_2$); 1274 (N−O). UV/vis (CH_2Cl_2, 10^{-4} M, λ = nm; $\epsilon = 10^{-4}$ mol^{-1}·L·cm^{-1}): 342 (0.863); 278 (1.558); 221 (3.199). MS (ESI; MeOH) *m/z*: 328.2 [M + H]$^+$; 350.2 [M + Na]$^+$; 366.2 [M + K]$^+$. Anal. Calcd (%) for $C_{18}H_{21}N_3O_3$ (327.37 g/mol): C 66.04; H 6.47; N 12.84. Found: C 65.84; H 6.51; N 12.70.

4-Methoxy-2-[*N*′-(2,6-diisopropylphenylimino)carbaldimine]pyridine *N*-Oxide (6). Adapted from the literature.[26] Under an inert atmosphere, to a solution of 4-nitro-2-iminomethylpyridine *N*-oxide (**5**, 500 mg, 1.5 mmol) in dry methanol (5 mL) was added dropwise a solution of MeONa (100 mg, 1.5 mmol) in dry methanol. The mixture was heated for 1 h at 40 °C, cooled, and hydrolyzed with water (20 mL). Extraction with CH_2Cl_2 afforded the product as a yellow solid (338 mg, 72%). Mp = 108.8 °C. ^{1}H NMR (300 MHz; $CDCl_3$; 298 K): δ 8.91 (s, 1H, CH═N); 8.13 (d, $^3J_{HH}$ = 7.2Hz, 1H, CH Py 2); 7.68 (d, $^4J_{HH}$ = 3.3 Hz, 1H, CH Py 3); 7.14 (m, 3H, Ar-p and -o); 6.91 (dd, $^3J_{HH}$ = 7.2Hz; $^4J_{HH}$ = 3.3 Hz, 1H, CH Py 5); 3.94 (s, 3H, O-CH$_3$); 2.88 (m, 2H, CH(CH$_3$)$_2$); 1,16 (d, 12H, CH(CH$_3$)$_2$). ^{13}C{^{1}H} NMR (75 MHz; $CDCl_3$; 298 K): δ 157.51 (1C, C$_q$-OMe Py 4); 155.63 (1C, CH═N); 148.43 (1C, C$_q$-CHN Py 2); 145.94 (1C, C$_{ipso}$ Ar); 141.12 (1C, CH Py 6); 137.47 (2C, C$_q$-CH(CH$_3$)$_2$); 125.27 (1C, CH Ar-p); 123.39 (2C, CH Ar-o); 115.18 (1C, CH Py 5); 108.02 (1C, CH Py 3); 56.57 (1C, O-CH$_3$); 28.26 (2C, CH(CH$_3$)$_2$); 23.74 (2C, CH(CH$_3$)$_2$). IR (Nujol): ν 1619 (C═N); 1591 (C═N); 1298 (OMe); 1193 (N−O). UV/vis (CH_2Cl_2, 10^{-4} M, λ = nm, $\epsilon = 10^{-4}$ mol^{-1}·L·cm^{-1}): 388 (0.372); 293 (1.422); 243 (2.697); 226 (3.267). MS (ESI; MeOH) *m/z*: 313.2 [M + H]$^+$; 335.2 [M + Na]$^+$; 351.2 [M + K]$^+$. Anal. Calcd (%) for $C_{19}H_{24}N_2O_2$ (312.40 g/mol): C 73.05; H 7.74; N 8.97. Found: C 73.19; H 8.10; N 8.39.

General Procedure for NiBr$_2$(PymNox) Complexes. To a solution of (dme)$NiBr_2$ (308 mg, 1 mmol) in CH_2Cl_2, quickly filtered to a cooled Schlenk (−20 °C), was added dropwise the corresponding ligand (1.1 mmol). After stirring at room temperature for 30 min the mixture was concentrated and the product was precipitated by addition of hexane. Filtration and washing with hexane (3 × 15 mL) afforded the product as a powder.

(Me,H)NNO-NiBr$_2$, Ni1. The reaction of **1** (326 mg, 1.1 mmol) with $NiBr_2$(dme) afforded the product **Ni1** as a red-brown powder (386 mg; 75%). ^{1}H NMR (300 MHz; CD_2Cl_2; 298 K): δ 27.7 (1H, $\Delta\nu_{1/2}$ = 15 Hz; CH Py); 21.8 (2H, $\Delta\nu_{1/2}$ = 27 Hz, CH Ar); 21.1 (1H, $\Delta\nu_{1/2}$ = 28 Hz, CH Ar); 11.9 (2H, $\Delta\nu_{1/2}$ = 440 Hz, CHMe$_2$); 4.2 (6H, $\Delta\nu_{1/2}$ = 22 Hz, CHMeMe); 1.4 (6H, $\Delta\nu_{1/2}$ = 59 Hz, CHMeMe); −5.9 (1H, $\Delta\nu_{1/2}$ = 26 Hz, CH Py); −16.7 (1H, $\Delta\nu_{1/2}$ = 26 Hz, CH Py); −17.4 (1H, $\Delta\nu_{1/2}$ = 25 Hz, CH Py); −26.7 (3H, $\Delta\nu_{1/2}$ = 33 Hz, CH$_3$). IR (Nujol, ν cm^{-1}): 1617.6 (C═N); 1213.3 (N−O). UV/vis (CH_2Cl_2, 10^{-4} M, λ = nm, $\epsilon = 10^{-4}$ mol^{-1}·L·cm^{-1}): 234.21 (2.00). Magnetic moment μc = 3.48 μ_B. Anal. Calcd (%) for $C_{19}H_{24}Br_2N_2NiO$ (514.91 g/mol): C 44.32; H 4.70; N 5.44. Found: C 45.01; H 5.02; N 5.29.

(H,H)NNO-NiBr$_2$, Ni2. The reaction of **2** (310 mg, 1.1 mmol) with $NiBr_2$(dme) afforded the product **Ni2** as a red powder (400 mg; 80%). IR (Nujol, ν cm^{-1}): 1632.5 (C═N); 1209 (N−O). UV/vis (CH_2Cl_2, 10^{-4} M, λ = nm, $\epsilon = 10^{-4}$ mol^{-1}·L·cm^{-1}): 324 (0.40); 283 (0.784); 241 (1.90). MS (ESI, CH_2Cl_2/MeOH) *m/z*: 421.1 [NiBr(1)]$^+$. Magnetic moment μc = 3.28 μ_B. Anal. Calcd (%) for $C_{18}H_{22}Br_2N_2NiO$ (500.88 g/mol): C 43.16; H 4.43; N 5.59. Found: C 43.29; H 4.82; N 5.71.

(H,Qui)NNO-NiBr$_2$, Ni3. The reaction of **3** (332 mg, 1.1 mmol) with $NiBr_2$(dme) afforded the product **Ni3** as a green powder (418 mg; 76%). ^{1}H NMR (300 MHz; CD_2Cl_2; 298 K): δ 23.1 (1H, $\Delta\nu_{1/2}$ = 76 Hz, CH Py); 14.2 (1H, $\Delta\nu_{1/2}$ = 61 Hz, CHMeMe); 11.9 (1H, $\Delta\nu_{1/2}$ = 30 Hz, CH Ar); 11.0 (1H, $\Delta\nu_{1/2}$ = 64 Hz, CHMeMe); 8.9 (3H, $\Delta\nu_{1/2}$ = 98 Hz, CHMeMe); 8.5 (1H, $\Delta\nu_{1/2}$ = 20 Hz, CH Qui); 8.2 (1H, $\Delta\nu_{1/2}$ = 20 Hz, CH Qui); 7.7 (2H, $\Delta\nu_{1/2}$ = 74 Hz, CH Ar); 5.0 (3H, $\Delta\nu_{1/2}$ = 73 Hz, CHMeMe); 4.0 (3H, $\Delta\nu_{1/2}$ = 85 Hz, CHMeMe); 3.4 (3H, $\Delta\nu_{1/2}$ = 98 Hz, CH Qui); 2.7 (1H, $\Delta\nu_{1/2}$ = 24 Hz, CH Qui); 2.0 (3H, $\Delta\nu_{1/2}$ = 49 Hz, CHMeMe); −15.9 (1H, $\Delta\nu_{1/2}$ = 56 Hz, CH Py). IR (Nujol, ν cm^{-1}): 1703, 1629, 1613, 1307, 1254 (N−O), 1196, 1140, 1102, 887, 748, 722. UV/vis (CH_2Cl_2, 10^{-4} M, λ = nm, $\epsilon = 10^{-4}$ mol^{-1}·L·cm^{-1}): 325 (0.57); 277 (1.55); 258 (1.77); 223 (3.18). Magnetic moment μc = 3.44 μ_B. MS (ESI, CH_2Cl_2 + MeOH) *m/z*: 801.2 [NiBrL2]$^+$; 469 [NiBrL]$^+$; 333.2 [L + H]$^+$. Anal. Calcd (%) for $C_{22}H_{24}Br_2N_2NiO$ (550.94 g/mol): C 47.96; H 4.39; N 5.08. Found: C 47.64; H 4.94; N 4.75.

(H,Ph)NNO-NiBr$_2$, Ni4. The reaction of **4** (358 mg, 1.1 mmol) with $NiBr_2$(dme) afforded the product **Ni4** as a pink powder (502 mg; 90%). ^{1}H NMR (300 MHz; CD_2Cl_2; 298 K): δ 31.2 (1H, $\Delta\nu_{1/2}$ = 30 Hz, CH Py); 21.0 (2H, $\Delta\nu_{1/2}$ = 45 Hz, CH Ar); 17.7 (1H, $\Delta\nu_{1/2}$ = 71 Hz, CH Ar); 11.9 (2H, $\Delta\nu_{1/2}$ = 213 Hz, CHMeMe); 10.6 (2H, $\Delta\nu_{1/2}$ = 30 Hz, CH Ph); 8.7 (1H, $\Delta\nu_{1/2}$ = 24 Hz, CH Py); 4.5 (6H, $\Delta\nu_{1/2}$ = 35 Hz, CHMeMe); 2.37 (6H, $\Delta\nu_{1/2}$ = 61 Hz, CHMeMe); 0.5 (2H, $\Delta\nu_{1/2}$ = 30 Hz, CH Ph); −11.4 (1H, $\Delta\nu_{1/2}$ = 44 Hz, CH Py); −14.4 (1H, $\Delta\nu_{1/2}$ = 33 Hz, CH Py). IR (Nujol, ν cm^{-1}): 1630; 1599; 1408; 1315; 1278; 1234; 1205 (N−O); 1166; 1101; 763. UV/vis (CH_2Cl_2, 10^{-4} M, l = nm, $\epsilon = 10^{-4}$ mol^{-1}·L·cm^{-1}): 336 (0.87); 289 (1.73); 250 (2.53). Magnetic moment μc = 3.52 μ_B. MS (ESI, CH_2Cl_2 + MeOH) *m/z*: 495 [LMBr]$^{+\cdot}$ Anal. Calcd (%) for $C_{24}H_{26}Br_2N_2NiO$ (576.97 g/mol): C 49.96; H 4.54; N 4.86. Found: C 49.53; H 4.69; N 4.51.

(H,H,NO2)NNO-NiBr$_2$, Ni5. The reaction of **5** (360 mg, 1.1 mmol) with $NiBr_2$(dme) afforded the product **Ni5** as a brown powder (408 mg; 75%). IR (Nujol, ν cm^{-1}): 1628, 1606, 1583, 1345, 1277, 1255 (N−O), 1198, 1167, 1074, 951, 932, 811, 758. UV/vis (CH_2Cl_2, 10^{-4} M, λ = nm, $\epsilon = 10^{-4}$ mol^{-1}·L·cm^{-1}): 338 (0.40); 275 (0.48); 223 (3.2). Magnetic moment μc = 2.93 μ_B. Anal. Calcd (%) for $C_{18}H_{21}Br_2N_3NiO_3$ (545.87 g/mol): C 39.60; H 3.88; N 7.70. Found: C 40.08; H 4.66; N 7.39.

(H,H,OMe)NNO-NiBr$_2$, Ni6. The reaction of **6** (312 mg, 1.1 mmol) with $NiBr_2$(dme) afforded the product **Ni6** as a brown powder (451 mg; 85%). IR (Nujol, ν cm^{-1}): 3318, 1637, 1613, 1489, 1310, 1191, 1165, 1107, 1022, 944, 796. UV/vis (CH_2Cl_2, 10^{-4} M, λ = nm, $\epsilon = 10^{-4}$ mol^{-1}·L·cm^{-1}): 331 (0.69); 283

Table 4. Polymer Yields and Activities for Ethylene−Methylacrylate Copolymerization

entry	Ni, μmol	Al/Ni	comon. addn. time, min[a]	reaction time, h	polym yield, mg	activ.[b]
1	4	1000	3	2	30	4
2	4	1000	3	2	30	4
3	10	800	1	3	650	22
4	10	800	1	24	800	3

[a] Delay for comonomer introduction after MMAO addition. [b] kg/mol Ni·h.

(1.06); 240 (2.74). Magnetic moment $\mu c = 3.22\ \mu_B$. MS (ESI, CH_2Cl_2 + MeOH) *m/z*: 763.1 $[NiBrL2]^+$; 451 $[NiBrL]^+$; 313.2 $[L + H]^+$. Anal. Calcd (%) for $C_{19}H_{24}Br_2N_2NiO_2$ (530.90 g/mol): C 42.98; H 4.56; N 5.28. Found: C 43.13; H 5.08; N 5.44.

(H,Ph)NNO-PdCl$_2$, Pd4. A mixture of ligand **4** (0.5mmol; 179.2 mg) and $PdCl_2$ (0.5 mmol; 88 mg) in CH_3CN was stirred at 40 °C for 4 h. After removing the solvent under vacuum, the solid was washed with hexane (2 × 15 mL) and then dried under reduced pressure. **Pd4** was obtained as a yellow powder (240 mg, 90%). ^{1}H NMR (300 MHz; CD_2Cl_2; 298 K): δ 8.06 (dd, $^3J_{HH} = 8.4$ Hz, $^4J_{HH} = 4$ Hz, 2H, H o-Ph); 7.98 (t, $^3J_{HH} = 7.6$ Hz, 1H, H Py 4); 7.93 (dd, $^3J_{HH} = 7.6$ Hz, $^4J_{HH} = 2$ Hz, 1H, H Py 5); 7.89 (s, 1H, CHN); 7.74 (dd, $^3J_{HH} = 7.6$ Hz, $^4J_{HH} = 2$ Hz, 1H, Py 3); 7.59 (m, 3H, H m and p Ph); 7.34 (t, 1H, H p Ar); 7.22 (d, 2H, H m Ar); 3.53 (m, 2H, CH iPr); 1.50 (d, $^3J_{HH} = 6.4$ Hz, 6H, Me iPr a); 1.19 (d, 6H, Me iPr b, $^3J_{HH} = 6.4$ Hz). ^{13}C{^{1}H} NMR (100 MHz; CD_2Cl_2; 298 K): δ 156.84 (1C, CHN), 153.40 (1C, Cipso Ph); 145.37 (1C, Cq Py2); 142.06 (1C, Cq Py6); 140.42 (2C, Cq-iPr); 133.71 (1C, CH p Ph); 132.47 (1C, CH Py4); 132.13 (1C, CH Py3); 131.76 (1C, CH Py5); 130.62 (2C, CH o Ph); 129.10 (1C, Cipso Ar), 128.59 (2C, CH m Ph), 128.58 (1C, CH p Ar), 123.63 (2C, CH m Ar); 28.96 (2C, CH iPr); 24.31 (2C, Me iPr); 23.09 (2C, Me iPr). IR (Nujol, ν cm^{-1}): 1624; 1597; 1309; 1232; 1186; 971; 831; 808; 768; 696; 666. Anal. Calcd (%) for $C_{24}H_{26}Cl_2N_2OPd$ (535.80 g/mol): C 53.80; H 4.89; N 5.23. Found: C 54.01; H 4.95; N 5.45.

Polymerization Procedure. Typical homopolymerization reaction conditions: A Fischer Porter reactor was flushed with N_2, and the catalyst (4 or 10 mmol) was transferred in toluene (50 or 100 mL, respectively) and then charged with ethylene at the working pressure and temperature. When the pressure and temperature were stabilized, the reaction was started by addition of MMAO with a syringe. The temperature was maintained by a water bath and monitored during the experiment as well as the ethylene consumed. The experiment time was typically about 20 min. After that time the reaction was quenched by addition of 1 mL of a HCl/MeOH solution, and then the polymers were precipitated in a methanol solution.

Copolymerization Procedure. The reaction was set following the same protocol employed in homopolymerization, with 5 bar of ethylene pressure. Methyl acrylate (1 mL, 12 mmol) was injected with a syringe 1 or 3 min after MMAO. After the specified time the solvent was removed under vacuum, and the polymers were washed with aqueous HCl and extracted with CH_2Cl_2. Solvents were removed from this polymer solution in the rotary evaporator, and then the solid polymers were washed with methanol, filtrated, and finally dried under vacuum. Yields and catalytic activities are shown in Table 4. The NMR and IR spectra of the polymers are similar in all cases. One of the polymers (entry 4) was dissolved in CH_2Cl_2 and reprecipitated with THF in order to check the homogeinity of the product. The IR and NMR spectra of the sample were not altered by this procedure.

Crystal Structure Determination. A single crystal of suitable size, coated with dry perfluoropolyether was mounted on a glass fiber and fixed in a cold nitrogen stream, 100(2) K, to the goniometer head. Data collection was performed on a Bruker-Nonius X8Apex-II CCD diffractometer, using monochromatic radiation λ(Mo Kα_1) = 0.71073 Å, by means of ω and φ scans with a width of 0.30 and an exposure times of 10 to 30 s per frame, in the range $3.58° < 2\theta < 61.20°$, with a detector distance of 37.5 mm. The data were reduced (SAINT) and corrected for Lorentz−-polarization effects and absorption by multiscan method applied by SADABS.[32,33] The structure was solved by direct methods (SIR-2002)[34] and refined against all F^2 data by full-matrix least-squares techniques (SHELXTL).[35] All the non-hydrogen atoms were refined with anisotropic displacement parameters. The hydrogen atoms were included from calculated positions and refined riding on their respective carbon atoms with isotropic displacement parameters.

Crystal data for 1: $C_{19}H_{24}N_2O$, $M_r = 296.40$, colorless block crystal (0.28 × 0.15 × 0.15 mm^3) from chloroform; triclinic, space group $P\bar{1}$ (no. 2), $a = 8.5986(6)$ Å, $b = 8.6704(6)$ Å, $c = 11.4818(7)$ Å, $\alpha = 97.006(2)$, $\beta = 101.110(2)°$, $\gamma = 97.648(2)°$, $V = 822.85(10)$ Å^3, $Z = 2$, $\rho_{calcd} = 1.196$ g cm^{-3}, $F(000) = 320$, $\mu = 0.074$ mm^{-1}; 6663 measured reflections, of which 3957 were unique ($R_{int} = 0.0257$); 204 refined parameters, final $R_1 = 0.0473$, for reflections with $I > 2\sigma(I)$, $wR_2 = 0.1626$ (all data), GOF = 1.039.

Crystal data for 2: $C_{18}H_{22}N_2O$, $M_r = 282.38$, yellow plate crystal (0.50 × 0.22 × 0.20 mm^3) from hexane; monoclinic, space group $P2_1/n$ (no. 14), $a = 10.853(3)$ Å, $b = 22.624(5)$ Å, $c = 13.360(3)$ Å, $\beta = 101.549(6)°$, $V = 3214.1(12)$ Å^3, $Z = 8$, $\rho_{calcd} = 1.167$ g cm^{-3}, $F(000) = 1216$, $\mu = 0.073$ mm^{-1}; 25 438 measured reflections, of which 5955 were unique ($R_{int} = 0.0853$); 388 refined parameters, final $R_1 = 0.0535$ for reflections with $I > 2\sigma(I)$, $wR_2 = 0.1494$ (all data), GOF = 0.992.

Crystal data for 3: $C_{22}H_{24}N_2O$, $M_r = 332.43$, yellow prism crystal (0.28 × 0.26 × 0.13 mm^3) from diethyl ether/hexane; triclinic, space group P (no. 2), $a = 7.8275(3)$ Å, $b = 10.8435(3)$ Å, $c = 11.4514(4)$ Å, $\alpha = 104.8940(10)°$, $\beta = 101.5370(10)°$, $\gamma = 100.6490(10)°$, $V = 891.24(5)$ Å^3, $Z = 2$, $\rho_{calcd} = 1.239$ g cm^{-3}, $F(000) = 356$, $\mu = 0.076$ mm^{-1}; 22 670 measured reflections, of which 5385 were unique ($R_{int} = 0.0223$); 230 refined parameters, final $R_1 = 0.0429$ for reflections with $I > 2\sigma(I)$, $wR_2 = 0.1219$ (all data), GOF = 1.049.

Crystal data for 4: $C_{24}H_{26}N_2O$, $M_r = 358.47$, yellow prism crystal (0.50 × 0.44 × 0.42 mm^3) from hexane; orthorhombic, space group $P2_12_12_1$ (no. 19), $a = 11.3512(5)$ Å, $b = 13.2373(6)$ Å, $c = 14.0721(6)$ Å, $V = 2114.46(16)$ Å^3, $Z = 4$, $\rho_{calcd} = 1.126$ g cm^{-3}, $F(000) = 768$, $\mu = 0.069$ mm^{-1}; 24 863 measured reflections, of which 3175 were unique ($R_{int} = 0.0329$); 248 refined parameters, final $R_1 = 0.0434$ for reflections with $I > 2\sigma(I)$, $wR_2 = 0.1140$ (all data), GOF = 1.031.

Crystal data for 5: $C_{18}H_{21}N_3O_3$, $M_r = 327.38$, yellow prism crystal (0.50 × 0.08 × 0.07 mm^3) from diethyl ether/hexane; monoclinic, space group $P2_1$ (no. 4), $a = 9.0486(7)$ Å, $b = 6.0887(5)$ Å, $c = 15.6974(11)$ Å, $\beta = 99.066(3)°$, $V = 854.03(11)$ Å^3, $Z = 2$, $\rho_{calcd} = 1.273$ gcm^{-3}, $F(000) = 348$, $\mu = 0.088$ mm^{-1}; 13 186 measured reflections, of which 1918 were unique ($R_{int} = 0.0309$); 221 refined parameters, final $R_1 = 0.0286$ for reflections with $I > 2\sigma(I)$, $wR_2 = 0.0697$ (all data), GOF = 1.037.

Crystal data for 6: $C_{19}H_{24}N_2O_2$, $M_r = 312.40$, yellow needle crystal (0.49 × 0.10 × 0.08 mm^3) from hexane; monoclinic, space group $P2_1/n$ (no. 14), $a = 7.7362(18)$ Å, $b = 6.0752(17)$ Å, $c = 35.758(9)$ Å, $\beta = 90.740(14)°$, $V = 1680.4(7)$ Å^3, $Z = 4$, $\rho_{calcd} = 1.235$ g cm^{-3}, $F(000) = 672$, $\mu = 0.080$ mm^{-1}; 20 686 measured reflections, of which 3807 were unique ($R_{int} = 0.0861$); 214 refined parameters, final $R_1 = 0.0773$ for reflections with $I > 2\sigma(I)$, $wR_2 = 0.2093$ (all data), GOF = 1.054.

(32) Bruker Apex 2, version 2.1; Bruker AXS Inc.: Madison, WI, 2004.
(33) Bruker. *SAINT* and *SADABS*; Bruker AXS Inc.: Madison, WI, 2001.
(34) SIR2002: Burla, M. C.; Camalli, M.; Carrozzini, B.; Cascarano, G. L.; Giacovazzo, C.; Polidori, G.; Spagna, R. *J. Appl. Crystallogr.* **2003**, *36*, 1103.
(35) *SHELXTL 6.14*; Bruker AXS, Inc.: Madison, WI, 2000−2003.

Crystal data for Ni1: $C_{40}H_{52}Br_4Cl_4N_4Ni_2O_2$, [$C_{38}H_{48}Br_4N_4Ni_2O_2$, $2(CH_2Cl_2)$], $M_r = 1199.72$, orange prism crystal ($0.31 \times 0.30 \times 0.21$ mm^3) from dichloromethane; monoclinic, space group *C*2/*c* (no. 15), $a = 20.3564(5)$ Å, $b = 10.6284(3)$ Å, $c = 21.7557(6)$ Å, $\beta = 94.3540(10)°$, $V = 4693.4(2)$ Å^3, $Z = 4$, $\rho_{calcd} = 1.698$ g cm^{-3}, $F(000) = 2400$, $\mu = 4.473$ mm^{-1}; 34 984 measured reflections, of which 7153 were unique ($R_{int} = 0.0256$); 253 refined parameters, final $R_1 = 0.0246$ for reflections with $I > 2\sigma(I)$, $wR_2 = 0.0636$ (all data), GOF = 1.024.

CCDC 683748−683754 contain the supplementary crystallographic data for this paper. These data can be obtained free of charge from The Cambridge Crystallographic Data Centre via www.ccdc.cam.ac.uk/data_request/cif.

Acknowledgment. Financial support from the DGI (Project CTQ2006-05527/BQU), Junta de Andalucía, and Repsol-YPF is gratefully acknowledged. We thank Dr. J. Angulo (IIQ) for recording two-dimensional DOSY spectra of copolymers.

Supporting Information Available: Full tables of bond and distance angles for the PymNox ligands, along with spectroscopic data for copolymers. This material is available free of charge via the Internet at http://pubs.acs.org.

OM800548Y